NASA Space Science Vision Missions

Edited by
Marc S. Allen

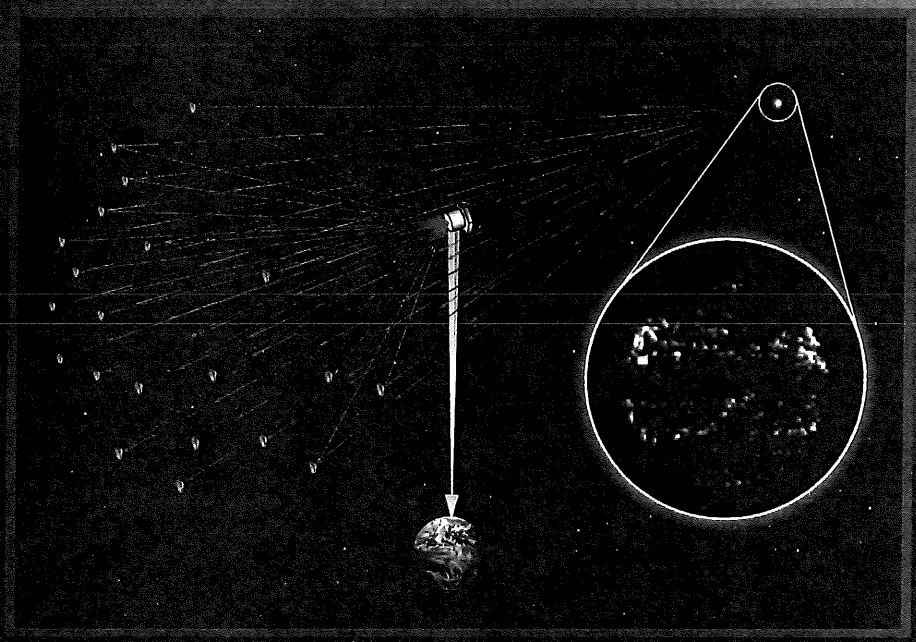

PROGRESS IN ASTRONAUTICS AND AERONAUTICS

Frank K. Lu, Editor-in-Chief
Volume 224

NASA Space Science Vision Missions

Edited by
Marc S. Allen
National Aeronautics and Space Administration
Washington, DC

Volume 224
PROGRESS IN
ASTRONAUTICS AND AERONAUTICS

Published by the
American Institute of Aeronautics and Astronautics, Inc.
1801 Alexander Bell Drive, Reston, Virginia 20191-4344

Chapter 5

Leaving the Heliosphere: A Nuclear-Powered Interstellar Probe

T. H. Zurbuchen,* P. Patel,† and L. A. Fisk‡
University of Michigan, Ann Arbor, Michigan

G. Zank§
University of California, Riverside, California

R. Malhotra¶
University of Arizona, Tucson, Arizona

H. O. Funsten**
Los Alamos National Laboratory, Los Alamos, New Mexico

and

R. A. Mewaldt††
California Institute of Technology, Pasadena, California

*Professor
†Graduate Student
‡Professor
§Professor, Director of Institute of Geophysics and Planetary Physics
¶Professor
**PhD, Director of the Center of Space Science and Exploration at LANL
††Senior Research Associate

I. Introduction

AN interstellar probe (ISP) constitutes the next logical step in the quest of humanity to explore the universe that surrounds us and of which we are a part. Our predecessors explored Earth's continents and crossed vast oceans at great peril. In the second half of the 20th century, we carried their spirit into space. This continuing need to explore has put humans on the Moon and has provided insights into our Solar System and the heliosphere in which it is embedded. The next logical step in this exploration is an ISP, a well-equipped spacecraft that will escape from the Sun's domain and enter our galactic neighborhood. The history of the Solar System is inextricably intertwined and determined by the evolutionary path taken by the Galaxy. The technical challenges posed by this quest are formidable. Getting to interstellar space in a reasonable time will require a spacecraft with unprecedented propulsion capability. This spacecraft must survive for decades and carry highly capable instruments that will continue to function long enough to complete its mission: explore the new frontier beyond the outer heliosphere.

This chapter details the results of one of two highly complementary technical approaches for an ISP that were funded under NASA's Vision Mission initiative. The study described here focuses on an ISP that utilizes nuclear reactor technology that is not currently available for use in space. This study explores the utility of nuclear technology, its challenges, and its effects on scientific instruments. When this study was initiated, NASA was aggressively pursuing such technologies, but those efforts have been reined in. The second study, led by McNutt et al.,[1] seeks to address this challenge using an entirely different and perhaps more promising approach given the current political and technological conditions. We first discuss our scientific objectives, the observations needed to achieve them, and their relation to NASA's strategic goals. We describe the scientific instruments, focusing on the status of the technology and the measurement and resource requirements for this mission, as well as the important effects of nuclear technology on space instrumentation. We discuss a multidimensional trade study that seeks to address the technological requirements that drive ISPs from the point of view of both propulsion and power. We then focus on one specific implementation of a nuclear-powered ISP that was studied using the Jet Propulsion Laboratory's (JPL) Team X process. This specific mission design reveals the current challenges to deployment and operation of such a system.

II. Science Rationale

The rapidly expanding solar atmosphere, the solar wind, creates a bubble called the heliosphere that shields our Solar System from the interstellar plasma and magnetic fields, as well as most of the cosmic rays and dust that comprise the local galactic neighborhood.[2–4] The proposed ISP will travel beyond the boundary of the heliosphere and, for the first time, explore the vast regions of our local galactic environment.

Figure 1 sketches the heliospheric boundary region as presently understood, based largely on theoretical considerations.[5,6] The region is composed of three distinct and rather well-defined boundaries. The innermost boundary is the

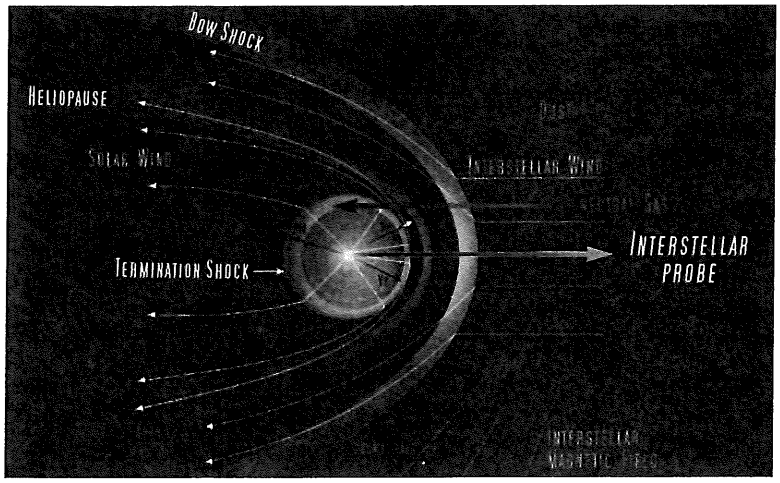

Fig. 1 An illustration of the structure of the heliosphere created when supersonic solar wind diverts the interstellar wind around the Sun. At the termination shock (~80–100 AU) the solar wind is slowed to subsonic values. The heliopause at around 120–150 AU separates solar material and magnetic fields from the interstellar material and fields. Of the spacecraft indicated (V1, Voyager 1; V2, Voyager 2; P10, Pioneer 10), only Voyagers 1 and 2 are still operating.

termination shock at around 95–100 AU. Because of its supersonic radial expansion, the solar wind is constantly thinning as it races away from the Sun, with a resulting pressure decrease of approximately $1/R^2$, where R is the heliocentric distance. The dynamic pressure falls until it becomes comparable to the interstellar pressure that forces the heliosphere into a bulletlike shape, which is shown in Fig. 1. There is therefore a transition point at which the supersonic solar wind becomes subsonic in response to this obstacle. After finishing their exciting interplanetary missions in 1989, the Voyager spacecraft embarked on a race to this solar wind boundary. In February 1998 Voyager 1 overtook Pioneer to become the outermost spacecraft ever built by humans. Finally, in December 2004 Voyager 1 crossed the termination shock.[7,8] The first measurements of this boundary have provided an important milestone in our understanding of the heliosphere and its interaction with the interstellar medium. However, these measurements have also exposed our lack of understanding of the key processes defining the structure of the termination shock and the highly dynamic heliosheath beyond. We will now discuss these new results.

The heliosheath, which represents the boundary of solar plasma, lies between the termination shock and the heliopause at around 120–150 AU. This boundary is expected to be rather well defined, because plasmas do not mix easily. The physical processes beyond the heliopause are determined by the properties of the interstellar medium, which are not well known. For example, the strength and vector direction of the interstellar magnetic field are unknown, even though there are creative ways to infer them from within our heliospheric bubble.[9] If the speed of the interstellar medium, measured relative to the Sun, is supersonic, we should expect an interstellar shock, where interstellar plasma is slowed and

deflected in an analogous fashion to the solar wind plasma ahead of the termination shock. That shock is expected to be located at around 180–200 AU. Beyond that, a spacecraft probing interstellar space will enter the vastness of our Galaxy.

An ISP is a mission to interstellar space. However, like the Voyager missions, an ISP will be a journey of exploration with a number of scientific discoveries cutting across the science disciplines of space physics, heliospheric physics, plasma physics, planetary physics, and, in using our heliosphere as an analog for other stellar heliospheres, astrophysics. The scientific importance of sending a spacecraft through this boundary region has been recognized by a number of studies,[10,11] as well as the 2002 Sun–Earth Connections Decadal Review. Similarly, the last two NASA Roadmaps and last two Strategic Plans, including the 2003 Strategic Plan, recommended this mission.[1] Thus far, a lack of sufficient advances in propulsion technologies has prevented an ISP from serious consideration for entering NASA's mission queue. With the potential availability of nuclear power and advanced propulsion technologies, our study suggests that such a mission is feasible without the need for other revolutionary technology development. The specific scientific rationales outlined here describe a mission that seeks to use an ISP as a flagship, taking a broad approach to exploration, without a narrow, specific focus. In this configuration, the ISP will be one of the most interdisciplinary missions ever conceived, addressing a wide set of discoveries across many different scientific fields.

The primary science objectives are described in Table 1. They are almost identical to the objectives in the 1999 NASA definition team report[12] (see also http://interstellar.jpl.nasa.gov/interstellar/probe/index.html), with the exception of objective 5, which is specific to this mission. The science objectives provide a natural sequence to the mission. Objective 5 can be addressed beyond 3 AU, objective 2 is of central importance at a heliocentric distance of 10 AU and beyond until, finally, objective 1 can be addressed beyond 150-AU heliocentric distances. This is sketched in Fig. 2, with specific science topics that will now be addressed in detail.

Table 1 Primary science objectives

Scientific objectives
1. Explore the nature of the interstellar medium and its implications for the origin and evolution of matter in our galaxy and the Universe
2. Explore the influence of the interstellar medium on the Solar System, its dynamics, and its evolution
3. Explore the impact of the Solar System on the interstellar medium as an example of the interaction of a stellar system with its environment
4. Explore the outer Solar System in search of clues to its origin and to the nature of other planetary systems
5. Explore the Universe from a unique vantage point beyond the zodiacal light and far from Earth

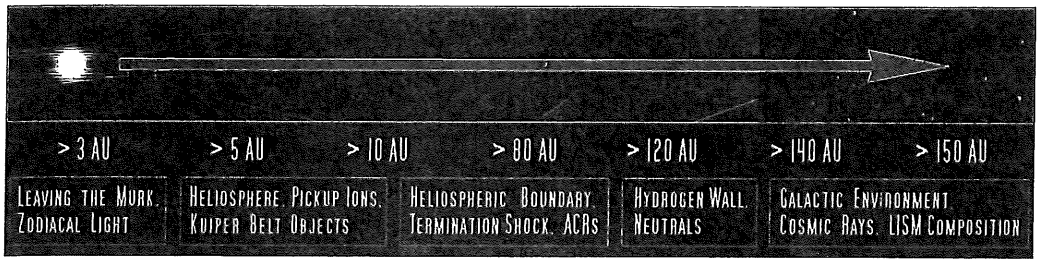

Fig. 2 The scientific objectives of the ISP at various distances along its trajectory.

A. Mission Science Objectives

1. Explore the Nature of the Interstellar Medium and Its Implications for the Origin and Evolution of Matter in Our Galaxy and the Universe

a. Current state of knowledge. The composition and physical processes governing the local interstellar medium (LISM) are constrained by both in situ and remote-sensing observations near the Sun.[13] Evidence of interstellar hydrogen and helium was initially provided by resonantly scattered ultraviolet (UV) light.[14] These observations, first made by Voyager and then the Solar Wind Anisotropies instrument on SOHO, provided crucial information about how interstellar neutral atoms travel through the heliosphere. These neutral He particles were directly measured at ~5 AU using the Ulysses Geostationary Atmospheric Sounder instrument. In this technique, particles are indirectly detected by their impact on an LiF target and subsequent sputtering and measurement of secondary ions,[15] which is sensitive for He but less so for H. The measurements resulted in an accurate determination of the flow vector and temperature of the interstellar medium. When interstellar neutrals are ionized in the heliosphere, for example, by photoionization, they are immediately subject to the electromagnetic forces of the solar wind, which sweeps the recently ionized particles into the far heliosphere. These so-called pickup ions (PICs) were detected by the Solar Wind Ion Composition Spectrometer on Ulysses, providing observations of densities and velocity-distribution functions of the pickup ions H^+, $^4He^+$, $^3He^+$, N^+, O^+, and Ne^+.[16–18] Such observations can also be made near 1 AU, for example, by the Advanced Composition Explorer (see references in Ref. 19). However, because the instruments measuring pickup ions were designed for measurement of the composition of the bulk solar wind rather than the tenuous flux of PICs, the statistical accuracy of the measurements is limited. Nevertheless, these measurements have substantially advanced our understanding of the neutral component of interstellar gas. These experimental results, combined with models and simulations of the heliosphere, have also provided parametric constraints for some plasma quantities, such as the magnetic field magnitude and direction in our local galactic neighborhood.[20] Unfortunately, these methods only provide insight into the neutral component of the interstellar gas, which is one of three major components of the interstellar medium, as shown in Fig. 3, which must be interpreted in concert. Furthermore, the neutral properties of H and O measured within the heliosphere are affected by filtration near the boundary caused by charge exchange. Except for He, there are few experimental

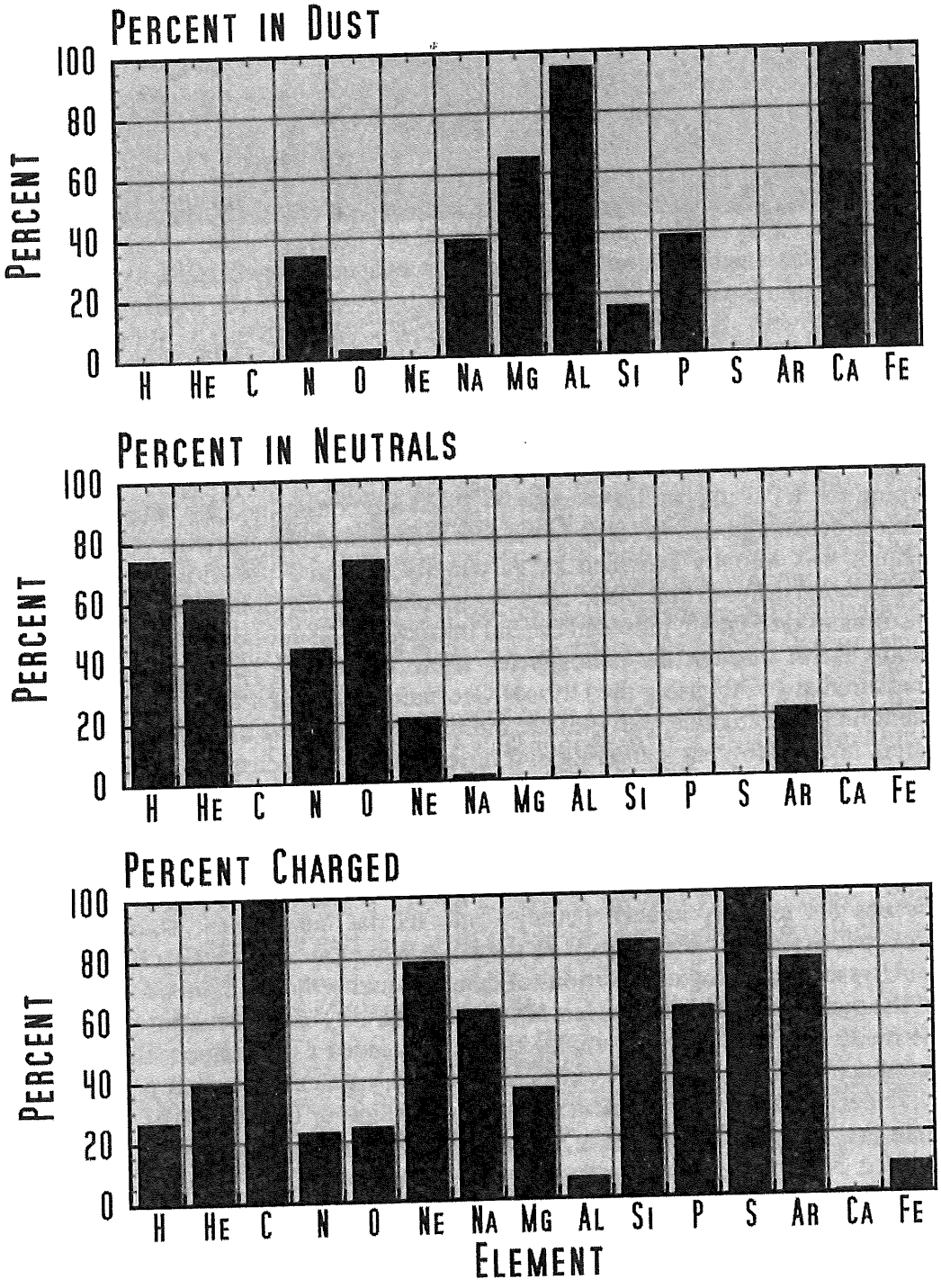

Fig. 3 The composition of the interstellar medium in dust, neutrals, and ionized components. All of these components need to be measured to determine the average composition of our galactic neighborhood.[26]

constraints on the isotopic composition of the interstellar medium, and our knowledge of the composition of the plasma and dust components of the LISM is likewise very limited.[21]

Like interstellar gas, energetic particles in the LISM also enter our heliosphere (Ref. 3 and references therein). However, unlike interstellar neutrals, these energetic particles immediately react to the structure and dynamic behavior of the heliosphere. For many years the studies of the transport of galactic cosmic rays (GCRs) have tended to focus on the region within the heliosphere.[22] It is now clear that the boundary region beyond the termination shock constitutes at least half of the modulation effect of the heliosphere in its entirety.[23,24] After crossing the termination shock, Voyager 1 collected GCR spectra that still show significant modulation, and the actual shape of the pristine cosmic ray spectrum in our LISM is not clear.[7,8]

b. ISP key science. Measure the composition of interstellar neutral gas, plasma, and the dust component: One of the most important goals of the ISP is to make the first comprehensive measurements of the composition of all significant components of the LISM. The LISM is composed of three different states: neutral, ionized, and dust components, as shown in Fig. 3.[25,26] Elements like C, S, and Si are predominately in a plasma state and, because of their low ionization potential, ionized. Elements such as H, N, He, and other noble gases are predominantly neutral and therefore in a gas phase; these have been observed, in part, as they enter the heliosphere, because they are not affected by the electromagnetic forces of the heliosphere and its boundary. Other elements, such as Al, Ca, Mg, and Fe, are mostly condensed in dust grains.

The physics of the LISM can only be assessed when these three states are combined and interpreted together. Low mass elements, such as H, He, and Li, are expected to have originated from the Big Bang, with specific abundance ratios dependent on, and representative of, the early evolution of the universe. Most other elements were and still are being created by nucleosynthesis in stars and subsequently ejected into interstellar space by stellar winds, similar to the wind generated by our Sun, or through the violent ends of stars in supernova explosions. The local cloud includes younger material than that of the presolar nebula and should therefore be richer in heavier elements and isotopes that have been generated by ongoing nucleosynthesis.

The neutral atom, ion, and dust components are literally samples of stars and stellar evolution that we seek to measure. An accurate and complete analysis of all three components will provide the most important ground truth for our understanding of the evolution of stars. They will provide a snapshot of our galaxy's history and a definitive test of our theoretical models that describe the cosmological evolution of our Galaxy and, by extension, the Universe.

Measure the nature of the local interstellar magnetic field and low-energy galactic cosmic rays: The LISM is expected to carry a magnetic field and with it a highly nonthermal plasma distribution, extending to high energies. We do not know much about the mean magnetic field of the LISM, its three-dimensional (3-D) orientation,[20,27] or the turbulent component. The magnetic field, together with the plasma components, determines the plasma properties of the LISM, as well as the Mach number of the flow relative to the Sun, which is important because it will decide whether there is an interstellar bow shock and because it

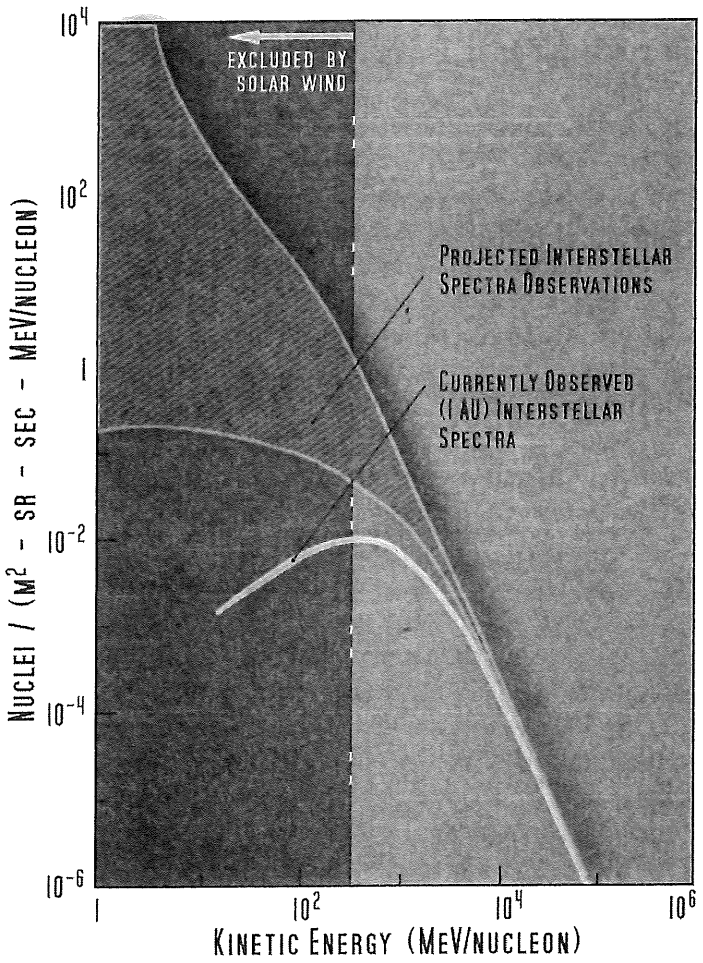

Fig. 4 The range of possible energetic particle distributions in the local interstellar medium. Low-energy particles are excluded by the solar wind. The lowest level curve indicates observations in the solar wind.

dominates the nature of the dynamic interaction between the heliosphere and interstellar space. This analysis will provide important clues about the processes that heat and ionize the interstellar medium.

The energetic ions and electrons of the LISM originate from astrophysical processes that include shock acceleration and the acceleration of these particles in the magnetically structured Galaxy. There is a large uncertainty in the distribution of these energetic ions and electrons, as demonstrated in Fig. 4. The pristine (unmodulated) spectrum can be measured only after penetrating beyond the entire boundary region shown in Fig. 1.

2. *Explore the Influence of the Interstellar Medium on the Solar System, Its Dynamics, and Its Evolution*

a. Current state of knowledge. The interstellar medium interacts with the heliosphere in many different ways. The ionized component and its magnetic field

influence the size of the heliosphere. Neutral atoms, high-energy GCRs, and some dust enter the heliospheric boundary and shape its overall structure, even modifying its size.

There are a number of key measurements that have shaped our understanding of the governing processes. The probability that interstellar neutrals will be ionized as they enter the heliosphere is strongly dependent on their heliocentric distance.[3] When they become ionized, they gyrate about the solar wind magnetic field and are then entrained within the solar wind that is radially expanding away from the Sun.[28] This pickup process effectively converts some kinetic energy of the bulk solar wind to the thermal energy of these ions. This tends to decrease the effective Mach number of the outer heliosphere, therefore directly affecting how perturbations propagate.[29] Beyond 10–15 AU, the internal energy, or pressure, of the heliospheric plasma is dominated by PICs, and the dynamic evolution of the solar wind, its turbulence, and its magnetic field are affected, as shown by Ulysses and Voyager.[30] PICs are swept out in the solar wind and, through a process that is not currently understood, are further accelerated in the heliospheric boundary region. These so-called anomalous cosmic rays (ACRs) are a crucial test of our understanding of particle acceleration processes in astrophysics: we know the source, and until the Voyager observations we thought we knew the region of acceleration, but can we predict their spectral shape and evolution?

Our knowledge of the termination shock of the solar wind, and the heliosheath beyond, has increased dramatically with the crossing of the termination shock by Voyager 1 on 16 December 2004 at 94 AU from the Sun.[7,8,31,32] This passage marks a major milestone in the exploration of space and the beginning of a new adventure: an exploration of the heliosheath beyond the termination shock. Although Voyager observations are relatively primitive, with instruments designed and built in the 1970s, these observations have revealed a number of surprises.

The most important constraint provided by Voyager 1 is simply the location of the termination shock. Predictions of the location of the termination shock have varied over the years but, with improved understanding of the conditions in the LISM, they have centered on 90–100 AU from the Sun (as reviewed by Stone[33]). Because the location of the termination shock depends not only on the solar wind ram pressure, which is measured, but also on the magnetic field and gas pressure of the LISM, knowing that the shock is located at 94 AU provides an important constraint on models for the interaction of the heliosphere with the LISM.

There have also been great expectations for the termination shock as the acceleration site for ACRs. ACRs are considered to originate from interstellar neutral gas that is swept into the Solar System by the motion of the Sun relative to the LISM. This gas is then ionized, picked up by the solar wind flow, and subsequently accelerated.[34] When these particles are first picked up by the solar wind they acquire energies on the order of 1 keV/nucleon. They are observed as ACRs at energies in excess of 10 MeV/nuc. Standard diffusive shock acceleration at the termination shock has long been considered a likely mechanism for accomplishing the required 4 orders of magnitude acceleration (see Refs. 3, 35, and 36 and references therein).

Perhaps the greatest single surprise at the shock crossing seen by Voyager was the absence of evidence for the acceleration of ACRs. Stone et al.[7] and Decker et al.[8] report that the intensity of the ACRs did not peak at the shock, indicating

that the source of the ACRs is not in the region of the shock local to Voyager 1. However, Decker et al.[8] do report dramatic increases in the intensity of low-energy (40–50 keV) ions at the shock and point out that these ions appear to have the same composition as interstellar PICs in that they are depleted of carbon. These accelerated, low-energy ions are also expected to originate as interstellar neutral gas, as do the ACRs, but have no obvious connection to the higher energy ACRs.

The spectra for the low-energy ions accelerated at the termination shock have a strikingly uniform spectral shape observed downstream of the termination shock.[7,8] The spectra of the downstream particles are power laws. When expressed as differential intensity versus particle energy, the spectral index is −1.5, or when expressed as a distribution function versus particle velocity, the spectral index is −5. This constant spectral shape persists throughout the observed heliosheath.

The spectral shape of energetic particles in the heliosheath is identical to the common spectrum observed for energetic particles in the inner heliosphere and believed to result from stochastic acceleration in compressional turbulence.[37] A possible explanation for the particles observed downstream from the termination shock is that they experience a similar stochastic acceleration in the pronounced compressional turbulence observed in the heliosheath.[31] Such an explanation would imply that the higher energy ACRs are accelerated as part of this process; thus, their source lies deep in the heliosheath, making it important to continue the exploration of this region.

b. ISP key science. Measure the dynamic evolution of the solar wind and all its high-energy components: One important aspect of the ISP, unlike Voyager, is it will be equipped with instruments specifically designed to measure the key components of the solar wind, interstellar medium, and the interaction region that lies at their interface. Most important, it will measure the evolution of PICs, which has not been adequately described beyond the Ulysses observations at 5 AU.

Measure the structure and evolution of the heliospheric boundary: Voyager observations indicate that suprathermal ions and electrons of the solar wind play a crucial role in determining the structure of the termination shock and its related acceleration processes for ACRs. Complete understanding of the boundary region therefore has to include an experimental analysis of all dynamic components, including thermal plasma, PICs, suprathermal solar wind particles, ACRs, and waves. Understanding of the complex interplay of these dynamic components has direct relevance to particle acceleration in other astrophysical contexts, such as near astrophysical shocks.

3. *Explore the Impact of the Solar System on the Interstellar Medium as an Example of the Interaction of a Stellar System with Its Environment*

a. Current state of knowledge. The most dramatic impact the Solar System has on the interstellar gas is the creation of a so-called hydrogen wall, as modeled by magnetohydrodynamic models. One example is shown in Fig. 5.[38] The hydrogen wall refers to a significant enhancement of interstellar neutral hydrogen at the nose of the bullet-shaped interaction region because of a combination of the slowing down of the ionized component and the resonant charge exchange between neutral hydrogen and protons in this slow-down region. Direct observations of

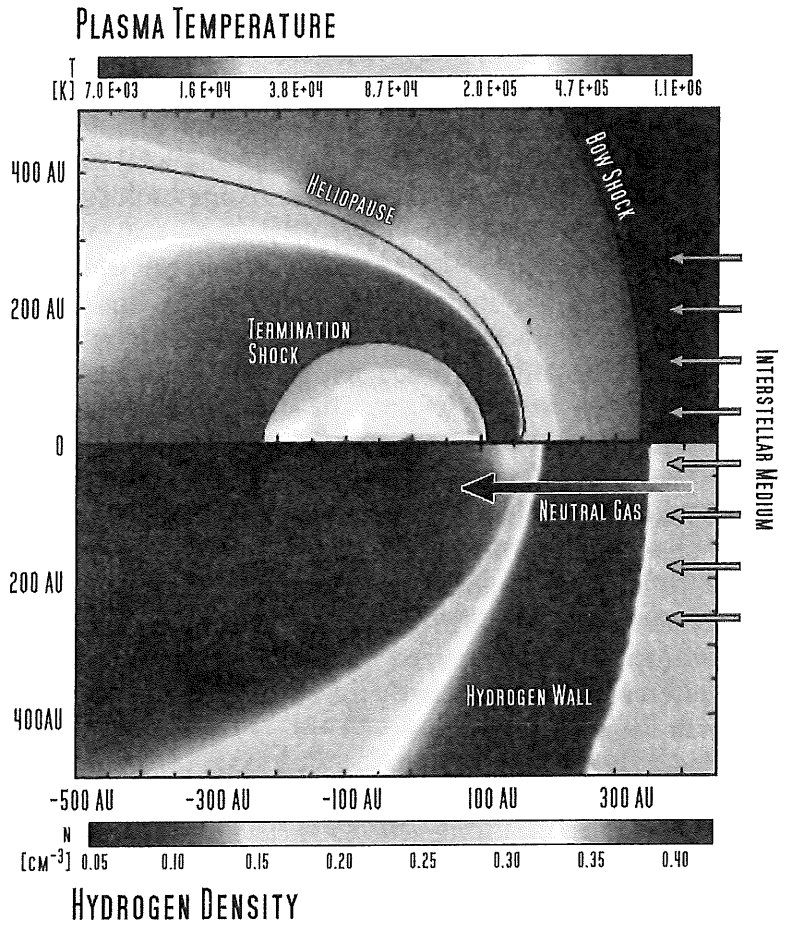

Fig. 5 The interaction region of the heliosphere with the Galaxy extends over a large range in heliospheric radius and can be observed remotely and in situ.

this wall were performed in 1996 by Linsky and Wood[39] using high-resolution spectral absorption measurements of H Ly-α UV (in the vicinity of 1216 Å). Excess UV absorption by the hydrogen wall is predicted by models such as the one shown in Fig. 5, because stellar Ly-α needs to pass through the enhanced H wall, which is also of elevated temperature, providing a very specific absorption signature. This technique has been applied to other stars and has provided the best evidence of solarlike stellar winds elsewhere.[40,41]

Another avenue for investigating the heliospheric boundary is through radio emissions observed in the outer heliosphere. Large solar perturbations have been observed to propagate through the outer heliosphere and the boundary region and surprisingly caused radio bursts at frequencies of 2–3 kHz that were detected onboard Voyager. These emissions are below the cutoff frequency of the solar wind in the inner heliosphere and at Earth and can only be observed from the outer heliosphere.[42–44] The frequency and timing signatures likely relate to the structure of that boundary region, but the current data are insufficient to infer this unambiguously.

Energetic neutral atoms (ENAs) also provide an avenue for exploring the heliosphere. These ENAs are accelerated in an ionized state and escape that

acceleration site after a charge exchange with the cold neutral atom component of the interstellar medium. Initial SOHO[45,46] measurements suggest that ENA creation exhibits a spatial dependence in the heliosphere. However, the interpretation of ENA maps is highly complex because of the long integration path involved. Local measurements acquired during travel through the interaction region will allow remote neutral atom imaging of the radial structure of this region.

b. ISP key science. Measure the properties of the hydrogen wall: The hydrogen wall is one of the most sensitive signatures of stellar winds. It is therefore important to quantify its physical processes and characterize their direct relation to the properties of solar and interstellar winds. This requires in situ measurement of the neutral atoms that form the wall as well as UV-absorption measurements during the passage by this wall.

Measure the properties of radio emissions in the heliospheric boundary: Radio emissions in the outer heliosphere will provide important remote-sensing tools that allow us to characterize the large-scale structure of the boundary regions, both in our Solar System and in others. It should also be noted that this frequency range of electromagnetic emissions in the Universe basically remains unexplored. The Voyager instrument is not optimized for detecting low-frequency emissions. Local wave measurements will also clarify the physical properties of the interstellar gas that is not at thermal equilibrium.

4. *Explore the Outer Solar System in Search of Clues to Its Origin and the Nature of Other Planetary Systems*

a. Current state of knowledge. The Solar System started as part of a complex stellar formation process originating in a protoplanetary nebula. In this process, angular momentum was exchanged through collisions and dynamic interactions between early Solar System bodies.[47,48] Signatures of this early history can still be observed today in the far regions of our Solar System, particularly in the Kuiper Belt beyond Pluto, as sketched in Fig. 6. Kuiper Belt objects (KBOs)

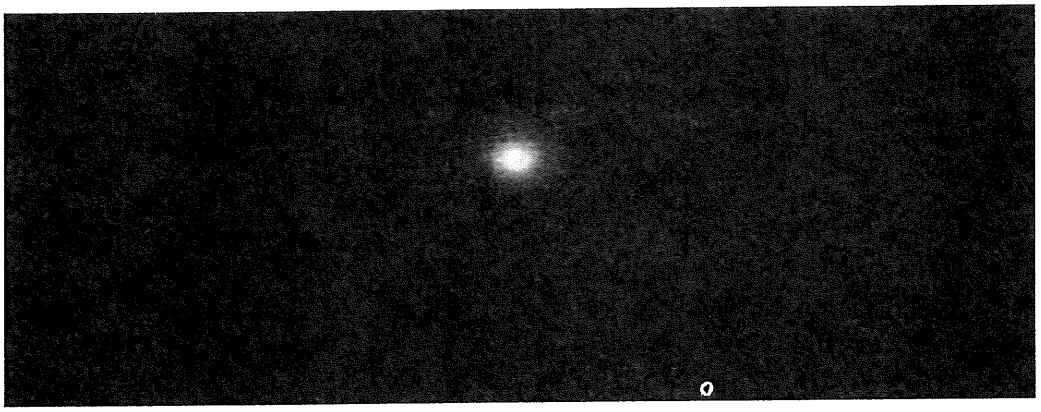

Fig. 6 An artist sketch of the Kuiper Belt (shown to scale) with orbits of planetary objects. The belt is highly structured, reflecting the dynamic evolution of the Solar System.

represent the early building blocks of the Solar System with imprinted signatures that reveal their evolutionary history. Progress in this field of research has been tremendous because of the improvement of Earth-based telescopes (e.g., Ref. 49 and references therein). KBOs are being discovered at an astonishing rate, and we now have sufficient statistics to start testing scenarios for the evolution of the Solar System. There is, for example, an enhanced likelihood of finding KBOs in resonance with Neptune. This probably resulted as gravitational interactions in the Solar System caused Neptune to migrate to larger heliocentric distance.[50]

A second source of matter in the outer Solar System is in the form of dust. This dust is a very close analog to planetary debris disks observed near other astronomical objects. These dust streams also affect the surfaces of small planetary bodies and the chemistry of the atmospheres of giant planets. Dust impacts were measured on Ulysses, Pioneer, and Voyager (see Ref. 51 and references therein). Ulysses and Galileo also provided measurements of interstellar dust grains that were detected based on their hyperbolic escape velocities (Refs. 52, 53, and references therein). The number of dust grains observed was unexpectedly high, with important potential consequences for objective 1 discussed above.

b. ISP key science. Measure the mass and orbit distribution of KBOs: KBOs can be observed from the outer heliosphere with optimal observational conditions and to lower masses than are possible from Earth in the near future, if ever. The distribution of small KBOs will allow us to address observational uncertainties, as discussed by Bernstein et al.[54] This will also constrain the radial extent of the primordial planetary disk.

Measure the distribution and composition of dust components in the outer Solar System: The dust components constitute the low end of the mass scale of planetary bodies in the outer Solar System. Detailed measurements will provide insights into the production mechanisms, which could be related to impacts of dust and KBOs or mutual collisions of KBOs. Dust composition measurements will also allow investigation of organic components. This topic has attracted substantial interest in the context of the origin of volatiles (including water) on Earth.

5. *Explore the Universe from a Unique Vantage Point Beyond the Zodiacal Light and Far from Earth*

a. Current state of knowledge. The zodiacal light of the inner heliosphere imposes a fundamental limit to observations in the infrared (IR) at wavelengths of <50 μm. This is a critical wavelength range for many reasons. Early galactic evolution has important signatures in the IR, and the cosmic ray IR background is expected to extend into this frequency range. Initial observations have been performed by the Cosmic Background Explorer and the zodiacal light limits were quantified by Reach et al.[55,56]

Many astronomical fields of research benefit from coordinated multipoint observations with a long baseline. This includes observations of parallaxes of stars and measurements of γ-ray bursts. Both will benefit from a baseline that is considerably larger than for any observations used to date.

b. ISP key science. Measure IR emissions from a vantage point beyond 10 AU: These observations are exploratory. They will provide insights relevant to the cosmic IR background and early galactic emissions.

Take advantage of the observational opportunities of a long baseline: Observations from the ISP will provide unique opportunities for multipoint observations. This includes long baseline observations of γ-ray bursts, for example.

B. Relation to NASA and Office of Space Science Strategic Plans

The ISP goes to the heart of the human urge to explore. The most recent strategic documents relevant to assess an ISP are the Heliophysics Roadmap (http://sec.gsfc.nasa.gov/Heliophysics_Roadmap.pdf) and the NASA Strategic Plan (http://www1.nasa.gov/pdf/142302main_2006_NASA_Strategic_Plan.pdf). Numerous reports of the National Research Council over the last decade have prioritized investments in an ISP, such as the latest decadal review of Space Science, "The Sun to Earth—and Beyond" (http://www.nap.edu/books/0309085098/html/R1.html), and the report on "Exploration of the Outer Heliosphere and the Local Interstellar Medium" (http://fermat.nap.edu/books/0309091861/html/R1.html).

An ISP is designed to understand the nature of our environment in space, consistent with the second of three science and exploration objectives (objective H) of the most recent heliophysics roadmap. As part of this, an ISP will identify key processes that couple the Sun and our planets to the heliosphere and beyond. It will make important contributions to our understanding of the transport of particles and how they are energized, and thus the impact of the interaction region on the Earth's space environment, as called out by objective F. It will make crucial observations of cosmic rays, the most important space weather hazard of long duration spaceflight, as is envisioned by the new Vision of Space Exploration put forth by President Bush in early 2004. Its results are therefore critical to objective J in the heliophysics roadmap.

The strength of an ISP, however, ranges far beyond heliophysics. There are fundamental science objectives related to the exploration of primitive bodies, highly prioritized in the latest National Research Council Decadal Survey for Solar System science. Furthermore, there are crucial science objectives in the realm of astrophysics. An ISP will address important topics related to the origin of the Universe as a whole, the origin of the Galaxy, and the properties of stars and their stellar winds.

Of the science objectives of the NASA Strategic Plan, an ISP makes critical contributions to two subgoals out of five (3B: Understand the Sun and its effect on Earth and the Solar System; 3C: Advance scientific knowledge of the origin and history of the Solar System). An ISP provides important supporting contributions to two additional subgoals (3D: Discover the origin, structure, evolution, and destiny of the Universe, and search for Earth-like planets; 3F: Understand the effects of the space environment on human performance, and test new technologies and countermeasures for long duration human space exploration).

C. Comparison with Alternatives

The alternatives for ISP mission concepts directly hinge on propulsion technologies that can enable them. Over the past few decades, four alternate approaches

have emerged that show promise to achieve the required spacecraft velocities while carrying the necessary scientific payloads. First, a spacecraft could be based on chemical propulsion.[57,58] To achieve a sufficiently high velocity, it needs to fly by Jupiter and the Sun, passing within 3 solar radii of the Sun's surface. A burn deep in the Sun's gravitational well will propel the spacecraft to high speeds. Second, the technology could be based on solar sail propulsion.[59] Solar sails are efficient close to the Sun, but the required sail properties are challenging.[60] The 1999 ISP study used a 25-kg payload having limited capability.[12] In order to deliver this payload a 200-m-diam sail with a total aerial density of 1 g/m^2, including support structures, must fly within 0.25 AU of the Sun. There is tremendous promise in solar sail technologies for a large array of space missions, and the development of such technologies may be beneficial in the long run. Third, McNutt and collaborators[1] suggest a radioisotope electric propulsion (REP) design, which also has very promising properties. Fourth, nuclear EP (NEP), the technology explored in this study, uses a nuclear reactor.[61–63] Compared to REP, NEP provides substantially more power, but with that comes a tremendous amount of technical complexity, which is discussed further in this chapter.

III. Architecture and Implementation Approach

A. Space Systems Architecture

The ISP Vision Mission study analyzed a variety of architectures, including those from the previous studies mentioned previously. The payload, data rates, and mission time line were modified to take full advantage of new technologies to fully exploit the science potential of a nuclear-powered ISP mission. In addition, technological trade studies were conducted to see how changes in the technologies would affect the mission and to provide a boundary on the minimum level of performance required. The principal technological goal of the ISP is to deliver a spacecraft to 150–200 AU within a 15–20 year time period. This timetable was chosen for direct comparison with the 1999 ISP study that used a solar sail. This distance and time frame is ambitious utilizing current propulsion and power technologies. To achieve the distance and time constraint requires the Solar System escape velocity to be at least a factor of 3 greater than Voyager 1's escape speed. Voyager 1 escaped the Solar System utilizing a combination of chemical propulsion and multiple gravity assists.

The baseline mission uses a nuclear-powered spacecraft, two daughtercraft, and suites of instruments to achieve the science and technical goals of the ISP mission. The nominal design is crafted around the Prometheus architecture. The study was performed by the JPL Team X design team in two separate sessions.

1. Mission Concept

For this ISP study an active nuclear reactor was selected as the power source, similar to Prometheus models. Consistent with a nuclear architecture, solar array technology was not utilized because it becomes useless in the outer heliosphere.

The baseline JPL Team X mission reaches 150 AU in 20.5 years, slower than the solar sail mission studied in 1999. However, the mass and power resources of the reactor-powered mission are dramatically larger. For example, the downlink

data rate from 200 AU is very large at 100 kbps. The launch date selected is 2 September 2025. A Jupiter gravity assist reduces the amount of propellant consumed and is therefore part of the baseline mission. The mothercraft carries a set of instruments and two daughter probes. The probes carry the most important instrument suite, focusing on the interstellar medium. Upon reaching 68 AU the mothercraft releases the probes to achieve a separation distance of >1 AU when crossing through the termination shock at around 95 AU. Utilizing multiple spacecraft substantially increases the scientific return of the mission because it helps resolve spatial–temporal ambiguities of dynamic events and structures and improves the reliability of the system to achieve the scientific goals of the mission. The Prometheus architecture, on which the design is based, allows for a 1500-kg science payload, thus enabling the ISP mission to carry two probes as well as a science suite aboard the mothercraft.

2. *Trajectory*

The trajectory optimization was conducted by selecting the power level and specific impulse and then optimizing the trajectory with the goal of achieving a heliocentric distance of 200 AU 20 years after launch. Out of the 21 candidate trajectories attempted during the Team X study, only one trajectory met the dry mass and launch vehicle escape energy C_3 constraint. The time of flight requirement was not met by the trajectory optimizer. Instead, the optimizer returned a trajectory that reached 150 AU in 20.5 years. The spacecraft launches on 2 September 2025 and arrives at 150 AU, the heliopause, after 20.5 years. The 200-AU mark is reached after a total of 26 years. The trajectory only has one thrust switching point. Thrusting begins after launch and ends 7.5 years later. After thrusting ends, the spacecraft simply coasts to 150 AU and beyond. Figure 7 shows the inner portion of the trajectory, and the arrows indicate the direction of thrust. The mission could be launched 5 years earlier if the Jupiter flyby is not utilized; however, the arrival date to 150 AU is almost unchanged, indicating that the Jupiter flyby offers sizable benefits in reducing the propellant mass, time of flight, and operations cost of this mission.

3. *Power and Propulsion System*

The baseline mission uses an active nuclear power source in conjunction with EP. Because of the nature and limits of the study much of the important information on reactors and related technologies was restricted. Instead, a simple scaling law was prescribed by the Prometheus team, relating the primary power P_p from the reactor to the space system dry mass M_{dry}:

$$M_{\text{dry}}\,[\text{kg}] = 10{,}800\,\text{kg} + 50\,\text{kg} \times P\,[\text{kWe}]. \tag{1}$$

No attempt was made to rationalize the model, for example, by breaking the dry mass into its key subsystems. In addition, the scaling did not account for the payload module, the propellant, or the propellant tanks. The nominal power level found is 125 kW. Assuming the EP system is 70% efficient, the jet power of the engines is 88 kW. The propulsion system utilized xenon propellant at a

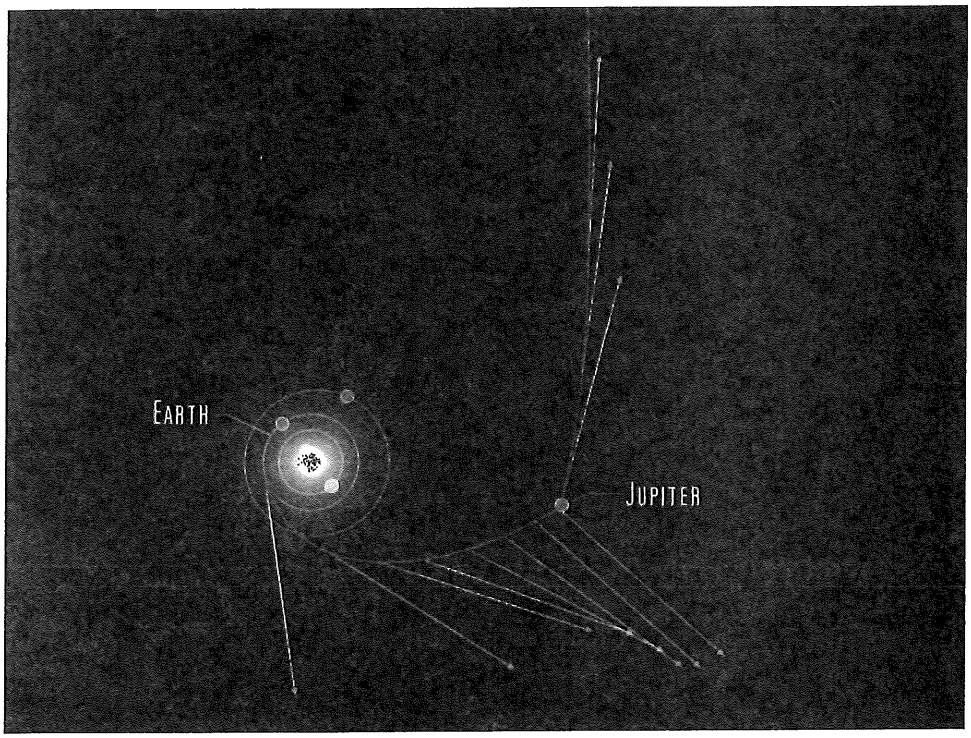

Fig. 7 The ISP trajectory in the inner heliosphere. Arrows indicate thrust vectors. The planetary configuration is provided for scale.

specific impulse of 5000 s. The specific impulse is achievable utilizing current technology.[64,65]

4. *Launch Vehicle*

Due to the large mass suggested by Eq. (1), current launch vehicles are inadequate to launch the reactor and provide the necessary Earth escape energy C_3. Currently, the maximum C_3 of 0 km^2/s^2 launch mass achievable is ~9300 kg (Delta IV Payload Planner's Guide, http://www.boeing.com/defense-space/space/delta/guides.htm). The large reactor mass and the time constraint necessitate the use of a Saturn V class launch vehicle. The Saturn V class launch vehicle's mass and C_3 relationship was provided by JPL to aid the study. A large positive C_3 is required to minimize the time to 200 AU. The optimized design point requires that the launch vehicle provide a C_3 of 56 km^2/s^2. The wet and dry masses of the spacecraft are 36,000 and 18,000 kg, respectively.

This by far exceeds any launch capability available today. It would require the development of a new launch vehicle or on-orbit assembly, which was selected as the baseline option. After the assembly, the spacecraft would have to be accelerated to a very large C_3 of 56 km^2/s^2 on a trajectory toward Jupiter. Note that the limitation comes from Eq. (1), which was not optimized in this study. Note also that there is a heavy lift launch vehicle development program planned (the Ares V) as part of NASA's program to return to the moon that may address this technological problem.

5. *Spacecraft Design*

The baseline mission design consists of the nuclear-powered mothercraft carrying a small suite of payload instruments with two additional probes. Both are shown in Fig. 8. The mothercraft (Fig. 8a) has a wet mass of 36,000 kg, broken down as 17,050 kg for the Prometheus spacecraft and 1500 kg for the mission module. The mothercraft is three-axis stabilized and has two EP thruster banks, each with four thrusters. The total thrust duration is 7.5 years, during which the engines consume 16,700 kg of propellant.

The two probes are autonomous spacecraft with a limited propulsion system. Figure 8b shows the baseline probe layout, with traditional body-mounted instruments and a deployed wave antenna. The probes use two multimission radioisotope thermoelectric generators (MMRTGs) to provide enough power at

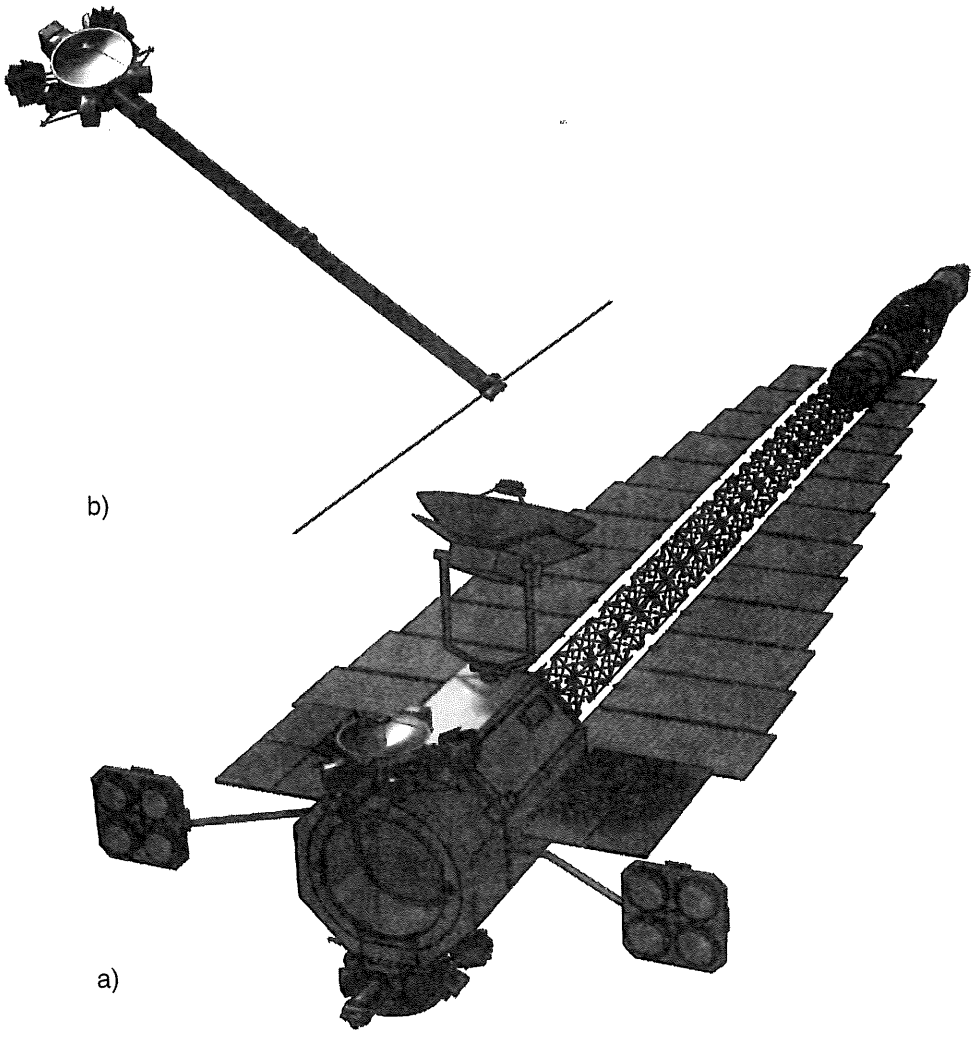

Fig. 8 The spacecraft design. The ISP mission is composed of one nuclear-powered mothercraft and two daughtercraft. a) The mothercraft with the two daughters in the stowed configuration, and b) the daughtercraft with deployed magnetometer and wave measurement.

end of life. The total power available at deployment is 480 W, and the power at 200 AU is 302 W. Utilizing one MMRTG and batteries was also explored; however, the battery lifetime was not sufficient for this mission. The total power required by the science payload is 17% of the available power. Data transmission to Earth requires a total of 158 W, enough for a data rate of 5 kbps using the Ka-band high gain antenna (HGA) at 100 AU. From 200 AU onward the direct to Earth data rate drops to 1 kbps. The required pointing accuracy is 0.1 deg., which is achieved by spinning the spacecraft at 1 rpm. Coning will be used as a secondary measure if the point requirement is not met. In order to prevent wobble a stepping motor with a mass is used to shift the center of gravity of the spacecraft. The probes carry a limited propulsion system to ensure that the spin axis is properly pointed toward Earth. The propulsion system will need to make corrections to the spin axis direction every 15 days. Each probe carries six hydrazine thrusters with a fuel mass of 10.05 kg. The probes will have to be autonomous because the one-way light travel time is >25 h at 200 AU.

B. Science Instrumentation

1. Overview

Figure 9 identifies the strawman instruments for the ISP. Most of these instruments have substantial heritage and were part of the 1999 ISP report.[12] The figure indicates how these instruments relate to the science objectives described in the previous sections. All instruments contribute to the breakthrough science of an ISP by making pioneering measurements in multiple phases of the mission. The first two sensors, magnetometer (MAG) and plasma and radio wave (WAV), measure electromagnetic radiation; the next three, solar wind electron (SWE), solar wind ion

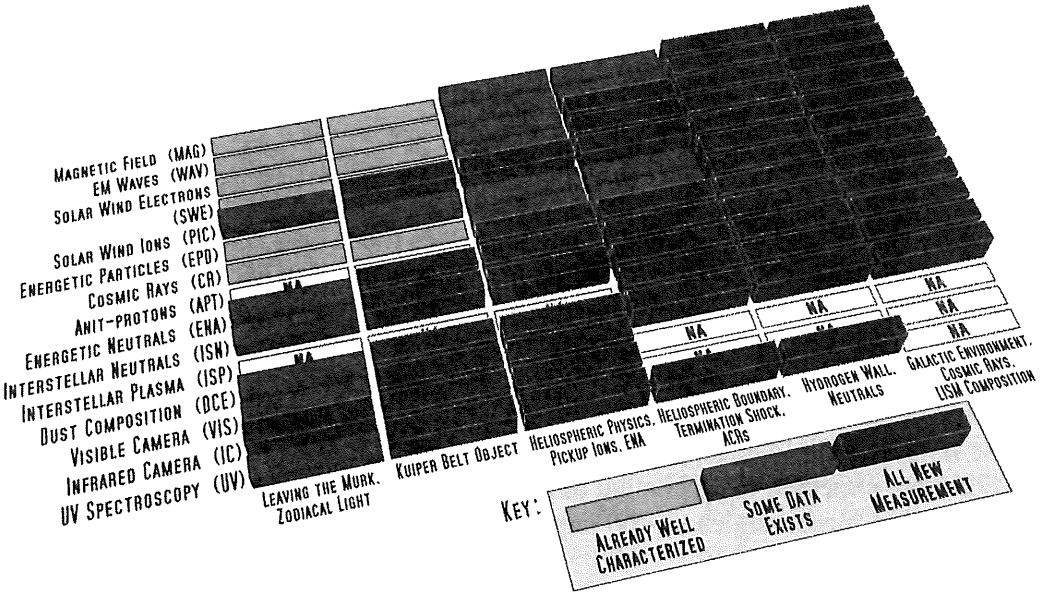

Fig. 9 Key instruments and their data. First measurements are indicated relative to the mission phases.

(SWI), and PIC, focus on solar wind measurements and the PICs in the heliosphere and its boundaries. A suite of energetic-particle instruments, energetic-particle detector (EPD), cosmic ray (CR), and antiproton telescope (APT), provide energetic-particle measurement throughout the entire energy spectrum from suprathermal to relativistic energies. We have three instruments focused on neutrals and interstellar plasmas, interstellar neutral (ISN), interstellar plasma, and ENA. One instrument focuses on dust and its composition, dust composition experiment (DCE). The last three instruments provide remote-sensing information in the visible (VIS), IR, and UV spectral regions.

Because of the important effects of the nuclear reactor on the scientific instruments, the mission was designed to encompass a mothercraft and two identically instrumented daughters that would be released after most of the reactor burnout. The mothercraft includes the entire instrument suite listed in Fig. 9. The daughters include all in situ instruments, but the highly capable DCE is replaced with a simpler, lower resource instrument and cameras are not included (Table 2). Key development needs for these instruments are also discussed. The final part of this section summarizes the effects of the nuclear power system on these instruments.

2. *Electromagnetic Instrumentation*

Electromagnetic fields are measured by the ISP MAG and a WAV. Low-frequency magnetic fields in the outer heliosphere and interstellar medium are measured by the MAG. Constraints from Voyager data and model extrapolations predict fields on the order 0.01 nT, and a sensitivity of 0.001 nT is required. This is achievable with current technology, but it imposes important cleanliness constraints on the spacecraft and its systems.

The WAV instrument monitors low-frequency heliospheric emissions. It also surveys plasma waves in the outer heliosphere and interstellar space and supports the plasma instrumentation in providing accurate plasma density estimates. Finally, the plasma-wave instruments also detect dust in the outer heliosphere, as demonstrated by Voyager.

3. *Solar Wind Plasma and PIC Instruments*

Low-energy plasma measurements include all contributing plasmas and their composition. In the heliosphere, these instruments focus on SWE and SWI components from thermal to suprathermal energies. With increasing heliospheric distance, the PIC instrument measures the neutral atom component of the LISM after it has been ionized. Bulk SWIs are beamlike, lying within 45 deg. or less of the radial direction to the Sun, whereas PICs require a larger field of view of close to 2π sr centered in the solar direction. SWEs are observed from all directions, requiring a 4π sr field of view. During the transition through the heliospheric boundary, all particles are expected to be heated, increasing the angular acceptance requirement of the SWI to larger angles of ~60 deg. from the solar direction.

4. *Energetic Particles and Cosmic Rays*

This suite of instruments will provide measurements of the entire spectrum of energetic particles from suprathermal energies (EPD) to cosmic rays (CR).

Table 2 Instrumentation of the daughter probes

Name	Function	Mass	Power	Data rate, kbps	Data vol., kbits/day
	Field and wave instruments				
MAG	Magnetometer	1.8	3	0.15	12,960
WAV	Electric field measurement	7	15	1	86,400
SWI	Solar wind ions	6	5	0.3	25,920
SWE	Solar wind electrons	4	5	0.3	25,920
PIC	Pickup ion spectrometer	8	8	0.5	43,200
	Field and wave instrument totals	26.8	36	2.25	194,400
Plasma IPDU	Centralized data processing	10	12	0.05	4,320
	High energy instruments				
EPD	Energetic particle sensor	15	4	0.2	17,280
CR	Cosmic ray composition	12	10	0.4	34,560
APT	Antiproton detector	4	5	0.05	4,320
ENA	Energetic neutral atom imager	7	4	0.2	17,280
DUS	Dust counter	10	10	1	10
DCE	Dust composition experiment	15	15		320,000
ISN	Interstellar neutrals	8	8	0.5	43,200
ISP	Interstellar plasma	6	5	0.3	25,920
	High-energy instrument totals	77	61	2.65	462,570
Energetic IPDU	Centralized data processing	10	12	0.05	4,320
	Cameras				
VIS	Visible camera	30	40	3	259,200
IR	IR spectrometer	15	10	0.8	69,120
UV	UV camera with low-resolution spectroscopy	5	5	1	86,400
	Totals	173.8	176	9.75	1,080,330

The remote-sensing instruments and the high-resolution dust measurements (VIS, IR, UV, DCE) are solely part of the mothercraft.

Measurements include both electrons and ions, including ion composition. At the suprathermal energies, this also includes compositional measurements of the charge states of these ions. These instruments cover the energy range of 50 keV/nuc to 5 GeV, well into the cosmic ray energies. Higher energy measurements are not necessary because they can be successfully performed in the inner heliosphere. The payload also includes a low-energy (<200 MeV) APT. This measurement is crucial because it may provide important signatures of weakly interacting massive particles, one of the key candidates for the missing dark matter. These particles cannot enter the heliosphere because of modulation effects of the solar wind throughout the heliosphere. The high-energy instrument (CR) will also have the capability to detect γ-ray bursts.

5. *Interstellar Neutral and Plasma Components*

Neutral particle measurements become more and more critical as the ISP approaches the boundary regions. They make up key measurements addressing objective 1 on the composition of the interstellar medium, which also includes detailed measurements of the density enhancements related to the hydrogen wall. The interstellar plasma instrument will provide the first measurements of the properties of interstellar plasmas by looking in the ram direction. The speed of the ISP provides an important energy gain to these particles, increasing their detection efficiency, especially in the case of the ISN instrument. ENAs will be detected along the trajectory, providing topographic information on particle-acceleration sites in the heliospheric boundary regions.

6. *Dust Composition and Spatial Distribution*

This instrument consists of two sensors. The first one, the dust counter (DUS), provides a sufficiently large area to measure the mass distribution and direction of incidence of dust particles with adequate accuracy, as well as information about the elemental and isotopic composition of this dust. It is comparable to dust instruments currently in flight. It would provide the first direct measurements of dust in the distant Solar System, testing models of Solar System and exosolar debris disks.[66] A second sensor, yet to be developed, would provide breakthrough measurements of the organic composition of dust. This novel spectrometer (DCE) would allow dust to be captured without destroying its overall structure. It would then analyze the dust's molecular components, enabling breakthrough science. There are indications from remote observations of molecular clouds that structurally complicated molecules are astonishingly abundant. This includes polycyclic aromatic hydrocarbons (PAHs), which are possible building blocks for life. We currently do not know how to analyze PAHs, even in the vicinity of Earth.

7. *Remote Sensing Instruments*

Nobody would ever go for their first trip away from home and not bring a camera. The cameras planned for the ISP serve multiple purposes and are crucial to achieve the ISP measurement objectives. The IR camera (IC) consists of a very modest-aperture telescope (20 cm) with detectors covering wavelength bands from 5 to 150 μm. There is ample opportunity to improve this instrument to add higher resolution spectral capabilities. The IC instrument may need active cooling systems for which a lifetime of 15+ years may be difficult to achieve. The UV imager (UV) requires substantial spectral capability, with only limited spatial resolution. It has to have enough collecting power to see sufficiently accurate H Ly-α emissions generated by neutrals in the heliospheric boundary regions and in particular the hydrogen wall. These neutrals are expected to enter the outer heliosphere. Repeated scans of the sky perpendicular to the spacecraft velocity direction will allow a topographic analysis of the outer heliosphere and its boundary to interstellar space.

The visible camera (VIS) supports one of the most important tasks of the ISP mission in the outer heliosphere by detecting KBOs from 30 to 200 AU. These

images provide information about the mass of the distant Solar System, its distribution, and its dynamical state. The measurements provide important constraints on theories of the formation and dynamics of the Solar System. This design study investigated the possibility of using a novel photon-counting 2-D CMOS technology, integrally constructed with star masks and discriminators. This internal masking approach eliminates contamination from bright stars, dramatically reducing the signal/noise ratio, and hence enhancing detection of faint KBOs. This is a new technology with layered 3-D electronics. It is a very fast imaging system (>4000 fps) that could also take advantage of a flyby of a KBO, which, considering the large number of these objects now known, could be included in mission planning without adding significant constraints on the overall mission profile.

8. *Radiation Backgrounds*

The mission studied here uses nuclear electric power at around 200 kW electric (kWe). This power system generates energetic γ-ray and neutron radiation that can substantially affect backgrounds of scientific measurements. As part of this study, we have quantified these rates using key detector technologies. These include channel electron multipliers (CEMs) and microchannel plates (MCPs). These detectors are part of most in situ instruments, such as the sensors detecting SWIs and SWEs, interstellar plasmas and neutrals, and PIC instrumentation. They also could be part of the UV camera and the ENA instrument. Figure 10 shows the γ-ray flux at the payload, which is ~6×10^5 γ/cm²/s, although this flux and its

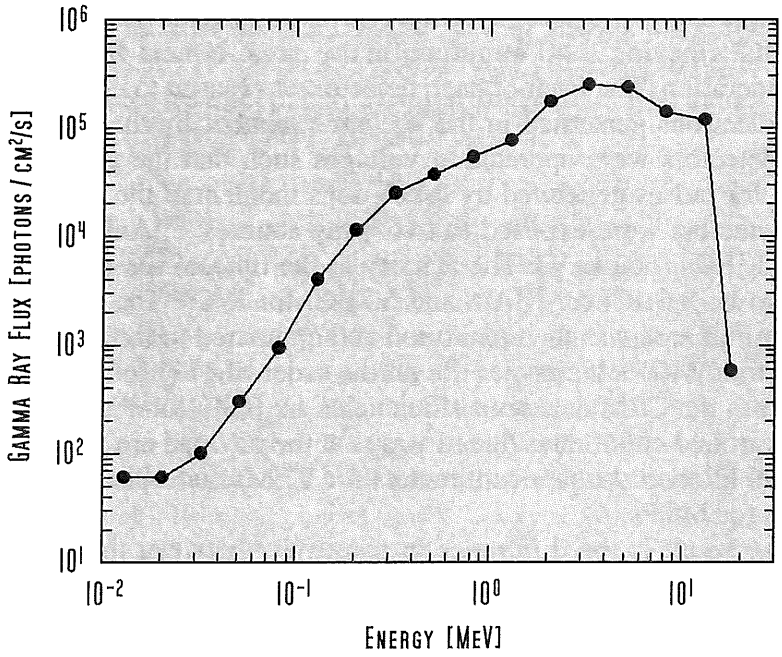

Fig. 10 The γ-ray flux from an 800-kWt reactor at a science payload located 25 m from the reactor. Calculations include 10-cm Be, 30-cm Li, and a simple Xe tank for shielding.

spectral distribution depends somewhat on the type and design of the reactor. In contrast, the total neutron flux at the payload for the same reactor and shielding conditions is 3×10^3 n/cm^2/s, and the neutrons interact less than γ-rays with the high-Z materials typically found in the instruments. The key challenges should therefore be expected from γ-rays.

The baseline reactor for the Vision Mission study is 200 kWe. Assuming that the conversion efficiency of thermal energy to electric energy is 25%, the required reactor is therefore 800 kW thermal power (kWt). Figure 10 shows the γ-ray flux for an 800-kWt reactor derived simply by doubling the flux calculated for a 400-kWt reactor. The total γ-ray flux at the payload, located 25 m from an 800-kWt reactor, is therefore 1.1×10^6 γ/cm^2/s. Electron-multiplier detectors such as CEMs and MCPs use electron multiplication to detect individual particles such as ions, electrons, neutral atoms, UV photons, or X-rays. Electron multipliers are sensitive to radiation that generates low-energy (less than several kiloelectron volts), secondary electrons along the multiplier's dynode surfaces, which subsequently initiate an electron avalanche in the multiplier and therefore a background count in the instrument. Because an operating nuclear reactor on a spacecraft produces penetrating radiation that loses energy to processes leading to production of low-energy electrons, instruments using electron-multiplier detectors are sensitive to this penetrating radiation. This background clearly has a direct impact on the signal/noise ratio of an instrument and therefore a measurement's statistical accuracy.

As part of this study we measured the sensitivity of CEMs and MCPs to penetrating γ-rays in order to understand the impact of the reactor on the performance of an instrument using these detectors. We analyzed these sensitivities using specific CEMs and MCPs currently in use. The Sjuts CEM had an input aperture area measuring 1.0×0.5 cm and a funnel area (i.e., area of the sensitive surface in the funnel) equal to 120 mm^2. The MCP detector consisted of a Z-stack of Burle MCPs having a 40-mm-diam active area, typical for the instruments under consideration. The front of each detector was biased to -120 V to repel any secondary electrons generated in the vacuum chamber by the γ-rays. The CEM and MCP detectors were operated at voltages such that the gain "plateau" was established for pulses generated by 2-keV ions incident at the front of the detectors. The detectors were exposed to two γ-ray sources: ^{241}Am (primary γ-ray at 60 keV) and ^{137}Cs (662 keV). The activity at the time of the measurements was calculated to be 9.6 μCi for ^{241}Am and 5.7 μCi for ^{137}Cs. The efficiency of each detector per unit area was then measured and compared to the incident γ-ray flux at the detectors. MCP efficiencies are on the order of 11% for ^{241}Am and 5% for ^{137}Cs, whereas the CEM detection efficiencies are 0.8% for ^{241}Am and 0.09% for ^{137}Cs. Background count rates due to γ-rays at the payload are therefore expected to be several kilohertz/square centimeters for CEMs and 10s of kilohertz/square centimeters for MCPs.

A striking result is the difference in sensitivity between the CEM and MCP detectors: the ratio of the MCP detection efficiency to that of the CEM was 15 for ^{241}Am and 35 for ^{137}C, making modern MCP detectors dramatically more prone to false counts than CEMs. This difference in detection efficiencies results from the different "active" areas of the detectors. For the CEM detector, an avalanche of sufficient magnitude to register a pulse can be generated in the funnel and at a small distance into the channel that is used for electron multiplication. The area of

the channel in which a secondary electron generated by a γ-ray can generate an avalanche is much less than the active area of the funnel. In contrast, an MCP is constructed using 1000s of parallel channels in the plate. As an example, a 1-cm^2 detector area of an MCP detector with MCPs having 8-μm-diam pores and 10-μm pitch (center–center spacing) has 10^6 channels and 25,100 mm^2 of channel area per millimeter of channel length. Although the distance into a channel from the front MCP detector surface at which an avalanche of sufficient magnitude can register a pulse is $\ll$1 mm, the active surface area intrinsic to the presence of so many channels in an MCP detector results in a much higher sensitivity to penetrating radiation than a CEM detector. This study is summarized in more detail by Funsten et al.[67]

These results suggest important consequences for shielding requirements or redesigns of scientific instruments, possibly relying more on traditional CEM technology instead of the more modern MCP technology. In any case, radiation background must be mitigated in these instruments.

IV. NEP Technology for ISP

The REP study performed by McNutt and collaborators[1] can be compared with this NEP study. These design points offer two specific solutions in our multidimensional design space. The REP approach uses a relatively low-power, high-C_3 solution. The spacecraft is relatively light in order to obtain a high C_3. The limited power in turn limits the amount of data that can be returned to Earth. The JPL design point uses a high-power, lower C_3 solution. Our NEP spacecraft is large and heavy because of the use of an active nuclear power system constrained by Eq. (1). Our NEP design has a total dry mass of 19,000 kg with a power of 125 kWe, whereas the REP design runs at <600 kg and 1 kWe, respectively. The two payload masses are 1500 and 35 kg, with very comparable payload/dry mass ratios. We have therefore undertaken a design study to look at the set of possible solutions of a nuclear-powered ISP system.

A. Assumptions

For this trade study several assumptions had to be made in order to limit the design space. The assumptions we made are related to the architecture of the mission. The parameters that are required before optimization can begin are the launch vehicle, propellant, efficiency curve, and gravity assist sequence/flyby altitude.

The launch vehicle selected for the study was the Atlas V 551. The Delta IV-Heavy Star variant or the Saturn V class launch vehicle model was not used because enough data about them did not exist to reliably use them in the optimization. The launch vehicle mass curves and C_3 curves were parameterized from the NASA Launch Vehicle Performance Web site (http://elvperf.ksc.nasa.gov/elvMap/staticPages/launch_vehicle_info1.html).

The JPL Team X study led to the conclusion that a Jupiter gravity assist is essential to enabling the ISP mission. Although multiple planetary flybys could offer greater payload mass fractions, they unduly constrain the launch dates and can adversely affect the time to 150 AU. For these reasons, only the Jupiter flyby is considered in the trade study. The flyby altitude selected is 4 Jupiter radii.

The amount of additional radiation shielding required is correlated to the flyby distance. Because this is unknown, it was decided to use a safer flyby altitude. For comparison, the JPL Team X design point utilized a flyby altitude of 1.5 Jupiter radii and the Johns Hopkins Applied Physics Laboratory led study utilized a flyby height of 1 Jupiter radius.

In addition, instead of arbitrarily selecting the efficiency of the EP engines, an efficiency model that captures the relationship between the specific impulse of the engines and the efficiency is used. Equation (2) describes the relationship between the specific impulse and the efficiency of the propulsion system.

$$\eta = \frac{\eta_{\max}}{1 + (\chi/c^2)}. \tag{2}$$

Here, $\eta_{\max}$ is assumed to be 71%, which gives a maximum efficiency of 75 and 95% for the EP engines and the power processing unit, respectively; and χ represents the specific ionization cost, which is assumed to be 10 times the first ionization energy of xenon. The exhaust velocity c is equivalent to

$$c = gI_{\text{sp}}, \tag{3}$$

where g is defined as $9.8\,\text{m/s}^2$ and the I_{sp} is the specific impulse of the EP engine (s).

We also assume that the propellant tank mass scales linearly with the propellant mass and that the structural mass scales linearly with the launch mass. In the trade study we assume that the tank mass is 10% of the propellant mass and the structural mass is 5% of the wet mass. The propellant selected for the study was xenon because krypton EP engines are currently not as efficient as xenon engines.[68]

The Earth and Jupiter orbits were assumed to be circular and coplanar. In addition, optimal phasing is assumed between the planets. The assumption about the planetary orbits allows the launch date to be found by simply searching for when the correct phasing between the planets occurs. Only the Sun is assumed to be gravitating, with gravity assists assumed to be instantaneous events that rotate the velocity vector.

The power level P is assumed to decay as

$$\frac{P(t)}{P_0} = \left(\frac{1}{2}\right)^{t/t_{1/2}}, \tag{4}$$

where $t_{1/2}$ is the half-life of the radioactive material. In the case of plutonium the half-life is 87 years. During the JPL Team X study the power from the reactor was assumed to be constant. We use the RTG power decay law because active nuclear reactors are not currently available, but RTGs are.

B. Methodology

The trade study optimized the power, propellant mass, and launch vehicle C_3 in order to maximize the payload mass fraction delivered to 150 AU in 20 years as a function of the reactor's mass/power ratio α. Optimizing the power level, propellant mass, and C_3 allows us to analyze the strong coupling between the launch

vehicle, the EP system, and the power system. The payload mass fraction is the mass not devoted to the power system, propellant, tanks, or structure, divided by the launch vehicle's mass at $C_3 = 0$ km^2/s^2. Normalizing the solution allows the system to scale. The problem was formulated as a calculus of variations approach utilizing optimal control theory. A homotopy method was then utilized to conduct the trade study. The algorithm is described in Patel et al.[69]

C. Results

Figure 11 represents the optimal mass fraction distributions for the various spacecraft systems. The JPL Team X design point sits significantly under the optimal solution due to the large fixed-mass cost of the nuclear reactor. Although each additional kilowatt of power costs 50 kg, the fixed cost of 10,800 kg inflates the α value, destroying any benefit gained from the scaling factor of 50 kg/kW. For power ranges of 50–200 kW, the α value of the reactor model varies from 266 to 104 kg/kW. The optimal specific impulses ranged from 15,000 to 10,000 s. EP engines in this range are not currently under development, but they have been investigated and are feasible.[64,65] As expected, lower αs lead to larger mass fractions, lower C_3 launches, and higher optimal specific impulses.

D. Conclusions for Nuclear-Powered ISP

From Fig. 11 we can draw several conclusions about the technology required to enable a fast ISP Mission. The trade space analysis indicates the need for low

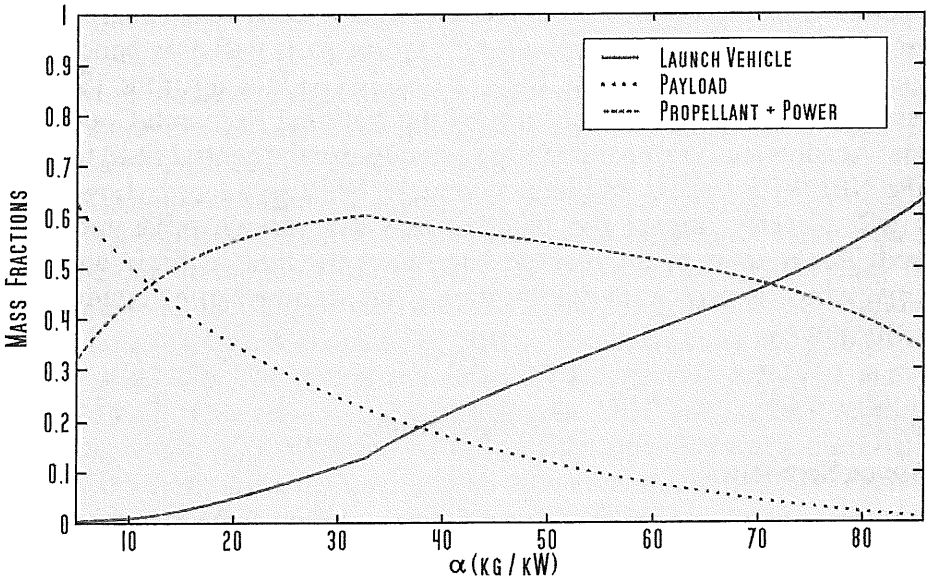

Fig. 11 A trade study of how the α value affects various spacecraft systems. As α increases, the payload mass fraction decreases whereas the launch vehicle C_3 increases. The JPL Team X design point represents the payload mass fraction of the ISP mission. If taken at face value, $\alpha_{JPL} \approx 130$ kg/kW, far beyond the optimization space used here. The maximum α for a viable mission occurs at around 70 kg/kW.

α and moderate specific-impulse systems. Alpha values from 30 to 70 kg/kW are required for a mission with performance comparable to the solar sail mission studied in 1999. NEP systems comparable to Prometheus have α values well over 150 kg/kW and are therefore not a feasible alternative. By comparing the launch vehicle curve and the power and propellant curve in Fig. 11, we can see that as α becomes larger the optimal solution favors using the launch vehicle over the EP system. This indicates that for large α values the system strongly depends on the launch vehicle rather than the EP system. Although the EP system still provides a benefit over a pure chemical system, the benefit is greatly diminished as α becomes large. Figure 11 also provides a boundary on what technology is required to obtain the goal of 150 AU in 20 years. We were not able to insert the JPL design point into Fig. 11 because it is well out of the range of possible mission designs for an ISP. In principle, we could add the design point by taking the 10,800-kg fixed reactor mass out of the payload allocation. In this case, the JPL design point would be approximately at $\alpha^*_{\text{JPL}} = 50\,\text{kg/kW}$, where α^* refers to the power scaling without that fixed mass. However, the payload reduces to 1.7% of the total launch vehicle capability, substantially smaller than outlined in Fig. 11. From Fig. 11 we see that the α values must be <70 kg/kW. This agrees with the independent findings of the National Research Council of the National Academies.[70] Because nuclear power benefits both the propulsion system and the communication system, this dual use allows nuclear designs to return orders of magnitude more data than a nonnuclear solution. To use current MMRTG technologies for the ISP mission would require relaxing the 150 AU in 20 years constraint to 150 AU in 25–30 years. Increasing the mission lifetime will create problems because most spacecraft systems are not designed to function for such long periods of time. This can lead to subsystems failing as the mission progresses, which can reduce the science or jeopardize the mission. In addition, decreasing the α will benefit all future nuclear missions whereas designing long-lifetime parts will only benefit a select few missions. In a larger context, the trade study conducted for the ISP mission addresses some of the issues put forth by the National Research Council of the National Academies.[70] From our study we recognize the central need to optimize both the NEP/REP system and launch vehicle. We also quantify how changing the α will directly impact the payload and the various other technologies involved. The α value of the reactor determines the time of flight and payload envelope, which is critical in determining what science can be conducted by a given mission.

V. Operations

A. Space Segment

The space operations consist of several phases. After launch, the spacecraft will undergo a 1-month on-orbit check out. The thrust phase then lasts for 7.5 years. After the thrust phase the spacecraft coasts and collects science data. The probes are then released and individually controlled. No interprobe communication is necessary.

The mothercraft's telecommunications system provides uplink and downlink capabilities. Data is transmitted to the Deep Space Network (DSN) via the

mothercraft's HGA at a data rate of 100 kbps at maximum range (200 AU). The link is designed to support this rate using 200 nodes (antennas) of the DSN 12-m antenna arrays (5 × 70 m equivalent aperture) at Ka-band with a 2.8-dB margin. If the multinode array is not ready in time to support the ISP mission, the telecommunications subsystem could implement an X-band downlink design using a single 70-m antenna, resulting in mass and power increases for the observatory.

The telecommunications system consists of four 100-W X-band traveling-wave tube amplifiers (TWTAs) and five 180-W Ka-band TWTAs using a 3-m-diam, gimbaled, HGA. The HGA is gimbaled to allow uplink and downlink functionality whereas the spacecraft is pointed toward the Sun to enable the long, continuous observation periods needed for the helioseismology objectives. Front and rear low gain antennas will be used for safing and command and control. The downlink safing data rate of 10 bps can be easily supported by the spacecraft. The uplink safing data rate of 7.8125 bps can be supported using a 20-kW uplink from a single 34-m-diam antenna (or arrayed equivalent).

The trade study analyzed two options for the probes' telecommunications systems. The first option is to directly downlink from the probes to the DSN. This allows the probes to act as autonomous vehicles with no interaction with the mothercraft. The data rate for a direct downlink to the DSN is 5 kbps to 200 × 12-m antennas in the Ka-band from 100 AU. The 5-kbps downlink rate will require a 3x compression scheme. The data rate drops to 1 kbps at 200 AU. This drop-off would necessitate the need for selectively downloading data or utilizing a better compression algorithm. To downlink the science data requires one 8-h pass/day. The probe utilizes a 1.5-m X-/Ka-band HGA for the primary direct to Earth communication leg. The power utilized by the telecommunication system is 158 W, and this requires the spacecraft to have a pointing accuracy of 0.1 deg. To achieve the pointing accuracy the probe spins at 1 rpm. A small stepping motor and mass are included in the design to control any wobble that may develop. The HGA is body fixed along the spin axis. The downlink margin for the direct to Earth link is 3.3 dB with a bit error rate of 10^{-6} at 100 AU.

The second option utilizes a link between the mothercraft and the probes. Each probe uses a UHF link to transmit the science data to the mothercraft that then transmits the data to the DSN. Using the UHF link does not require daily downlinks and allows all the science data to be returned to Earth. The UHF link uses a quad-helix antenna with a diameter of 20 cm. The antenna is body fixed with a beamwidth of 65 deg. The uplink and downlink frequencies are 437.1 and 401.5 MHz, respectively. One major issue with using the UHF link is that it requires the probes to be within 100–5000 km of the mothercraft. Although the UHF link returns all the science data, the issue of radiation contaminating the science needs to be analyzed further.

B. Ground Segment

The main purpose of the ground segment is to support a 20+ year mission to our local galactic neighborhood. The launch is in the 2020–2025 time frame, allowing the ground-system technology to evolve from today's status. In this study, it is

assumed that the future DSN 12-m, multinode antenna array (400-node implementation) is available. It should be noted that plans for the array deployment show the entire array (400 nodes at each site) being completed by fiscal year 2018, well before our projected launch date. Both X- and Ka-bands could be accommodated; our baseline is X-band. The ISP mission would also benefit from optical transmissions that may be available by the technology cutoff date.

The baseline plan allows for one downlink from the mothercraft per week, during which 910 MB will be downloaded. This requires onboard storage of 9 GB. Each daughtercraft also is tracked with one downlink per day with a total of 18 MB per downlink. Onboard storage requirements are below 1 GB. Direct downlink is used from each of the spacecraft. No interspacecraft communications are planned.

The ISP mission has three mission-critical, high-activity periods. The first is during the initial burn-out of Earth's gravitational well. The second phase is during a relatively close Jupiter flyby. The third phase is during the release of the daughtercraft. The first period is launch (L) to L+30 days. In this period, the spacecraft and nuclear power systems are checked out. The second period of continuous tracking is a 1-week period in support of trajectory determination during the Jupiter flyby. The third period of continuous tracking is 1 week in support of trajectory determination during probe drop-off.

VI. Risks and Safety

A. Nuclear Power System

It was generally agreed that the ISP mission design constitutes considerably less risk than the first mission in the Prometheus line, the Jupiter Icy Moons Orbiter (JIMO). The JIMO resilience and reliability requirements are comparable to this mission, but the engineering environments of JIMO are substantially more challenging. This includes the increased radiation dose in Jupiter's magnetosphere and the navigation and control requirements needed for orbit control in the near-polar orbits around Jupiter's moons.

B. Launch

Two launches are required for this mission: one to bring the carrier to low Earth orbit (LEO), another to carry the booster stage into LEO. The entire spacecraft then has to be assembled in orbit. After assembly, the booster injects the carrier spacecraft into its interplanetary trajectory, providing the necessary change in velocity. As soon as the booster stage is spent, it is jettisoned from the carrier spacecraft. The trajectory simulations assumed that the NEP system starts thrusting very soon after the booster is jettisoned, even though it is recognized that this may not be a realistic assumption.

The launch and near-Earth operations sequence has to be consistent with federal regulations about nuclear material and systems.

VII. Conclusions

Humanity has explored Earth and the space near us, and we are destined to go beyond the boundaries of our understanding and explore our galactic neighborhood

through an ISP. This team strongly believes that the technology enabling this mission will be associated with nuclear technology. It is not clear today whether it is going to be through means of radioelectric systems or through nuclear reactors, perhaps both.

When this Vision Mission was selected, Prometheus was apparently in a state of growth, with the promise to develop advanced nuclear propulsion and to bring us closer to our vision of interstellar exploration. At the time that this chapter was written, Prometheus was no longer a program with the promise to address this mission. Based on our study, the anticipated performance of the Prometheus nuclear power system would not match requirements adequate for its use for breakthrough missions like an ISP. However, the task at hand remains exciting and the motivation of the scientific community has not diminished for one of the most historic missions of exploration conceivable: the ISP.

Acknowledgments

We acknowledge contributions from the entire science team coming together in a meeting in Tucson, AZ, which was hosted by J. R. Jokipii. We also thank the team of engineers under the leadership of R. Oberto who performed the Team X system study at JPL. Particular thanks to M. Noca, C. Satter, and N. Murphy for support during this study. We thank M. Luna for documenting the Team X results. D. Eddy edited this paper with lots of patience and dedication, and the figures were provided by B. Grimm from Paper Cardinal Design (http://www.papercardinal.com/). We also acknowledge the contributions of the Nuclear ISP Vision Mission team: S. D. Bale, M. Brown, P. C. Frisch, A. Gallimore, K. Grogan, J. Holloway, M. Horanyi, J. R. Jokipii, P. C. Liewer, R. B. Lin, F. B. McDonald, N. Murphy, D. Poston, D. Scheeres, E. C. Stone, C. Sattler, and J. Vallerga.

References

[1]McNutt, R. L., Jr., Gold, R. E., Krimigis, S. M., Roelof, E. C., Gruntman, M., Gloeckler, G., Koehn, P. L., Kurth, W. S., Oleson, S. R., Leary, J. C., Fiehler, D. I., Anderson, B. J., Horanyi, M., and Mewaldt, R. A., "Innovative Interstellar Explorer," *Proceedings of the Solar Wind 11–SOHO 16 Conference Connecting Sun and Heliosphere*, edited by B. Fleck and T. H. Zurbuchen, Goddard Institute for Space Studies, New York, 2005, pp. 693–696.

[2]Parker, E. N., *Interplanetary Dynamic Processes*, Interscience Publishers, New York, 1963, pp. 118–121.

[3]Zank, G. P., "Interaction of the Solar Wind with the Local Interstellar Medium: A Theoretical Perspective," *Space Science Review*, Vol. 89, Nos 3–4, 1999, pp. 413–688.

[4]Zurbuchen, T. H., and Jokipii, J. R., "Picture of Outer Heliosphere Develops with New Data," *EOS Transactions*, Vol. 83, No. 44, 2002, pp. 499–503.

[5]Axford, W. I., "The Interaction of the SW with the Interstellar Medium," *Solar Wind*, edited by C. P. Sonett, P. J. Coleman, and J. M. Wilcox, NASA, Washington, DC, 1972, p. 609.

[6]Florinksi, V., Pogorelov, N. V., and Zank, G. P. (eds.), *Physics of the Outer Heliosphere, 3rd International IGPP Conference, AIP Conference Proceedings, Subseries: Astronomy and Astrophysics*, Vol. 719, Springer–Verlag, New York, 2004.

[7]Stone, E. C., Cummings, A. C., McDonald, F. B., Heikkila, B. C., Lal, N., and Webber, W. R., "Voyager 1 Explores the Termination Shock and the Heliosheath Beyond," *Science*, Vol. 309, No. 5743, 2005, pp. 2017–2020.

[8]Decker, R. B., Krimigis, S. M., Roelof, E. C., Hill, M. E., Armstrong, T. P., Gloeckler, G., Hamilton, D. C., and Lanzerotti, L. J., "Voyager 1 in the Foreshock, Termination Shock and Heliosheath," *Science*, Vol. 309, No. 5743, 2005, pp. 2020–2024.

[9]Lallement, R., Quémerais, E., Bertaux, J. L., Ferron, S., Koutroumpa, D., and Pellinen, R., "Deflection of the Interstellar Neutral Hydrogen Flow Across the Heliospheric Interface," *Science*, Vol. 307, No. 5714, 2005, pp. 1447–1449.

[10]Liewer, P. C., Mewaldt, R. A., "Interstellar Probe Using a Solar Sail," *Outer Heliosphere: The Next Frontiers*, edited by K. Scherer, Horst Fichtner, Hans Jörg Fahr, and Eckart Marsch, Vol. 11, Pergamon, Amsterdam, 2001, p. 411.

[11]Mewaldt, R. A., and Liewer, P. C., "Scientific Payload for an ISP Mission," *The Outer Heliosphere: The Next Frontiers*, edited by K. Scherer, Horst Fichtner, Hans Jörg Fahr, and Eckart Marsch, Vol. 11, Pergamon, Amsterdam, 2001, p. 451.

[12]Jet Propulsion Laboratory, "The Interstellar Probe Mission Architecture and Technology Report," JPL-D-18410, Oct. 1999.

[13]National Research Council, "Explorations of the Outer Heliosphere and the Local Interstellar Medium," Workshop Report, National Academy of Sciences, New York, 2004.

[14]Bertaux, J. L., and Blamont, J. E., "Evidence for a Source of Extraterrestrial Hydrogen Lyman-Alpha Emission: The Interstellar Wind," *Astronomy and Astrophysics*, Vol. 11, No. 2, 1971, pp. 200–217.

[15]Witte, M., Banaszkeiwicz, M., and Rosenbauer, H., "Recent Results on the Parameters of the Interstellar Helium from the Ulysses/GAS Experiment," *Space Science Review*, Vol. 78, Nos 1–2, 1996, pp. 289–296.

[16]Gloeckler, G., Geiss, J., Balsiger, H., Fisk, L. A., Galvin, A. G., Ipavich, F. M., Ogilvie, K. W., von Steiger, R., and Wilken, B., "Detection of Interstellar Pick-Up Hydrogen in the Solar System," *Science*, Vol. 261, No. 5117, 1993, pp. 70–73.

[17]Geiss, J., and Witte, M., "Properties of the Interstellar Gas Inside the Heliosphere," *Space Science Review*, Vol. 78, Nos 1–2, 1996, pp. 229–238.

[18]Gloeckler, G., and Geiss, J., "Abundance of ^{3}He in the Local Interstellar Cloud," *Nature*, Vol. 381, No. 6579, 1996, pp. 210–212.

[19]Russell, C. T., Mewaldt, R. A., and von Rosenvinge, T. T., *The Advanced Composition Explorer Mission*, Kluwer Academic, Dordrecht, 1998.

[20]Gloeckler, G., Fisk, L. A., and Geiss, J., "Anomalously Small Magnetic Field in the Local Interstellar Cloud," *Nature*, Vol. 386, No. 6623, 1997, pp. 374–377.

[21]Geiss, J., and Witte, M., "Properties of the Interstellar Gas Inside the Heliosphere," *Space Science Reviews,* Vol. 78, Nos 1–2, 1996, pp. 229–238.

[22]Jokipii, J. R., "The Physics of Cosmic-Ray Modulation," *Advances in Space Research*, Vol. 9, No. 12, 1989, pp. 105–119.

[23]Jokipii, J. R., Kota, J., and Merenyi, E., "The Gradient of Galactic Cosmic Rays at the Solar-Wind Termination Shock," *Astrophysical Journal*, Vol. 405, No. 2, 1993, pp. 782–786.

[24]McDonald, F. B., Heikkila, B., Lal, N., and Stone, E. C., "The Relative Recovery of Galactic and Anomalous Cosmic Rays in the Distant Heliosphere: Evidence for Modulation in the Heliosheath," *Journal of Geophysical Research*, Vol. 105, No. A1, 2000, pp. 1–8.

[25]Frisch, P. C., "Morphology and Ionization of the Interstellar Cloud Surrounding the Solar System," *Science*, Vol. 265, No. 5177, 1994, p. 1423.

[26]Frisch, P. C., and Slavin, J. D., "Chemical Composition and Gas-to-Dust Mass Ratio of Nearby Interstellar Matter," *Astrophysics Journal*, Vol. 594, No. 2, 2003, pp. 844–858.

[27]Frisch, P. C., "The Galactic Environment of the Sun," *American Scientist*, Vol. 88, No. 1, 2000, p. 52.

[28]Vasyliunas, V. M., and Siscoe, G. L., "On the Flux and the Energy Spectrum of Interstellar Ions in the Solar System," *Journal of Geophysical Research*, Vol. 81, Mar. 1, 1976, pp. 1247–1252.

[29]Lee, M. A., "The Termination Shock of the Solar Wind," *Space Science Review*, Vol. 78, Nos 1–2, 1996, pp. 109–116.

[30]Smith, C. W., Isenberg, P. A., Mattaheus, W. H., William, H., and Richardson, J. D., "Turbulent Heating of the Solar Wind by Newborn Interstellar Pickup Ions," *Astrophysical Journal*, Vol. 638, No. 1, 2006, pp. 508–517.

[31]Burlaga, L. F., Ness, N. F., Acuña, M. H., Lepping, R. P., Connerney, J. E. P., Stone, E. C., and McDonald, F. B., "Crossing the Termination Shock into the Heliosheath: Magnetic Fields," *Science*, Vol. 309, No. 5743, 2005, pp. 2027–2029.

[32]Gurnett, D. A., and Kurth, W. S., "Electron Plasma Oscillations Upstream of the Solar Wind Termination Shock," *Science*, Vol. 309, No. 5743, 2005, pp. 2025–2027.

[33]Stone, E. C., "News from the Edge of Interstellar Space," *Science*, Vol. 293, No. 5527, 2001, pp. 55–56.

[34]Fisk, L. A., Kozlovski, B., and Ramaty, R., "An Interpretation of the Observed Oxygen and Nitrogen Enhancements in Low-Energy Cosmic Rays," *Astrophysical Journal Letters,* Vol. 190, 1974, p. L35.

[35]Pesses, M. E., Eicher, D., and Jokipii, J. R., "Cosmic Ray Drift, Shock Wave Acceleration, and the Anomalous Component of Cosmic Rays," *Astrophysical Journal,* Vol. 246, June 1, 1981, pp. L85–L88.

[36]Jokipii, J. R., "The Anomalous Component of Cosmic Rays," *Physics of the Outer Heliosphere: Proceedings of the 1st COSPAR Colloquium*, edited by S. Grzedielski and D. E. Page, Pergamon, New York, 1990, pp. 169–178.

[37]Fisk, L. A., and Gloeckler, G., "The Common Spectrum for Accelerated Ions in the Quiet-Time Solar Wind," *Astrophysical Journal Letters*, Vol. 640, No. 1, 2006, L79–L82.

[38]Zank, G. P., and Pauls, H. L., "Modelling the Heliosphere," *Space Science Review*, Vol. 78, No. 1/2, 1996, pp. 95–106.

[39]Linsky, J. L., and Wood, B. E., "The Alpha Centauri Line of Sight: D/H Ratio, Physical Properties of Local Interstellar Gas, and Measurement of Heated Hydrogen Near the Heliopause," *Astrophysical Journal*, Vol. 463, 1996, p. 254.

[40]Wood, B. E., and Linsky, J. L., "The Local ISM and its Interaction with the Winds of Nearby Late-Type Stars," *Astrophysical Journal*, Vol. 492, 1998, p. 788.

[41]Wood, B. E., Linsky, J. L., and Zank, G. P., "Heliospheric, Astrospheric, and Interstellar Ly-α Absorption Toward 36 Oph," *Astrophysical Journal*, Vol. 537, No. 1, 2000, p. 304.

[42]Kurth, W. S., Gurnett, D. A., Scarf, F. L., and Poynter, R. L., "Detection of a Radio Emission at 3 kHz in the Outer Heliosphere," *Nature*, Vol. 312, Nov. 1, 1984, pp. 27–31.

[43]Gurnett, D. A., and Kurth, W. S., "Radio Emissions from the Outer Heliosphere," *Space Science Reviews*, Vol. 78, Nos 1–2, 1996, pp. 53–66.

[44]Gurnett, D. A., Kurth, W. S., and Stone, E. C., "The Return of the Heliospheric 2–3 kHz Radio Emission During Solar Cycle 23," *Geophysical Research Letters*, Vol. 30, No. 23, 2003, p. 2209.

[45]Hsieh, K. C., Shih, K. L., Jokipii, J. R., and Grzedzielski, S., "Probing the Heliosphere with Energetic Neutral Hydrogen Atoms," *Astrophysical Journal,* Vol. 393, No. 2, 1992, pp. 756–763.

[46]Hilchenbach, M., Hsieh, K. C., Hovestadt, D., Klecker, B., Gruenwaldt, H., Bochsler, P., Ipavich, F. M., Buergi, A., Moebius, E., Gliem, F., Axford, W. I., Balsiger, H., Bornemann, W., Coplan, M. A., Galvin, A. B., Geiss, J., Gloeckler, G., Hefti, S., Judge, D. L., Kallenbach, R., Laeverenz, P., Lee, M. A., Livi, S., Managadze, G. G., Marsch, E., Neugebauer, M., Ogawa, H. S., Reiche, K.-U., Schöler, M., Verigin, M. I., Wilken, B., and Wurz, P., "Detection of 55–80 keV Hydrogen Atoms of Heliospheric Origin by CELIAS/HSTOF on SOHO," *Astrophysical Journal,* Vol. 503, 1998, pp. 916–922.

[47]Weissman, P. R., "Source of Comets," *Science*, Vol. 269, No. 5227, 1995, p. 1120.

[48]Gladman, B., "The Kuiper Belt and the Solar System's Comet Disk," *Science*, Vol. 307, No. 5706, 2005, pp. 71–75.

[49]Jewitt, D., "KBOs," *Annual Review of Earth and Planetary Science*, Vol. 27, 1999, pp. 287–312.

[50]Malhotra, R., "The Origin of Pluto's Orbit. Implications for the Solar System Beyond Neptune," *Astronomical Journal*, Vol. 110, No. 1, 1995, p. 420.

[51]Landgraf, M., Liou, J.-C., Zook, H. A., and Grun, E., "Origins of Solar System Dust Beyond Jupiter," *The Astrophysical Journal*, Vol. 123, No. 5, 2002, pp. 2857–2861.

[52]Gruen, E., Gustafson, B., Mann, I., Baguhl, M., Morfill, G. E., Staubach, P., Taylor, A., and Zook, H. A., "Interstellar Dust in the Heliosphere," *Astronomy and Astrophysics*, Vol. 286, 1994, pp. 915–924.

[53]Gruen, E., Landgraf, M., Horanyi, M., Kissel, J., Kruger, H., Srama, R., Svedhem, H., and Withnell, P., "Techniques for Galactic Dust Measurements in the Heliosphere," *Journal of Geophysical Research*, Vol. 105, No. A5, 2000, pp. 10403–10410.

[54]Bernstein, G. M., Trilling, D. E., Allen, R. L., Brown, M. E., Holman, M., and Malhotra, R., "The Size Distribution of Trans-Neptunian Bodies," *The Astronomical Journal*, Vol. 128, No. 3, 2004, pp. 1364–1390.

[55]Reach, W. T., and Jeonghee, R., "Excitation and Disruption of a Giant Molecular Cloud by the Supernova Remnant 3C 39," *The Astrophysical Journal*, Vol. 511, No. 2, 1999, pp. 836–846.

[56]Reach, W. T., Franz, B. A., Weiland, J. L., Hauser, M. G., Kelsall, T. N., Wright, E. L., Rawley, G., Stemwedel, S. W., and Spiesman, W. J., "Observational Confirmation of a Circumsolar Dust Ring by the COBE Satellite," *Nature*, Vol. 374, No. 6522, 1995, p. 521.

[57]Jaffe, L. D., Ivie, C., Lewis, J. C., Lipes, R., Norton, H. N., Stearns, J. W., Stimpson, L. D., and Weissman, P., "An Interstellar Precursor Mission," JPL 77-70, 1977.

[58]Mewaldt, R. A., Kangas, J., Kerridge, S. J., and Neugebauer, M., "A Small ISP to the Heliospheric Boundary and Interstellar Space," *Acta Astronautica*, Vol. 35, January, 1995, pp. 267–276.

[59]Gavit, S. A., Liewer, P. C., Wallace, R. A., Ayon, J. A., and Frisbee, R. H., "Interstellar Travel—Challenging Propulsion and Power Technologies in the Next 50 Years," *Space Technology and Applications International Forum—2001*, edited by M. S. El-Genk, Vol. 552, American Institute of Physics, College Park, MD, 2001, pp. 716–726.

[60]Garner, C. E., Diedrich, B., and Leipold, M., "A Summary of Solar Sail Technology Developments and Proposed Demonstration Missions," AIAA Paper 99-2697, 1999.

[61]Patterson, M. J., Elliott, F., Malone, S., Soulas, G., Goebel, D., and Sengupta, A., "Herakles Thruster Development for the Prometheus JIMO Mission," *41st AIAA/ASME/SAE/ASEE Joint Propulsion Conference*, AIAA, Reston, VA, 2005, pp. 1–11.

[62]Oleson, S., "Electric Propulsion for Project Prometheus," *39th AIAA/ASME/SAE/ASEE Joint Propulsion Conference and Exhibit*, AIAA, Reston, VA, 2003.

[63]Dunning, J., and Jankovsky, R., "NASA's Electric Propulsion Program," *39th AIAA/ASME/SAE/ASEE Joint Propulsion Conference and Exhibit*, AIAA, Reston, VA, 2003.

[64]Foster, J. E., Haag, T., Kamhawi, H., Patterson, M., Malone, S., Elliot, F., Williams, G. J., Jr., Sovey, J. S., and Carpenter, C., "The High Power Electric Propulsion (HiPEP) Ion Thruster," *40th AIAA/ASME/SAE/ASEE Joint Propulsion Conference and Exhibit*, AIAA, Reston, VA, 2004.

[65]Oleson, S., Gefert, L., Benson, S., Patterson, M., Noca, M., and Sims, J., "Mission Advantages of NEXT: NASA's Evolutionary Xenon Thruster," *38th AIAA/ASME/SAE/ASEE Joint Propulsion Conference and Exhibit*, AIAA, Reston, VA, 2002.

[66]Moro-Martin, A., and Malhotra, R., "Dust Outflows and Inner Gaps Generated by Massive Planets in Debris Disks," *Astrophysical Journal*, Vol. 633, No. 2, 2005, pp. 1150–1167.

[67]Funsten, H. O., et al. "Comparative Response to Microchannel Plate and Channel Electron Multiplier Sectors to Gamma Ray," (in preparation).

[68]Linnell, J. A., and Gallimore, A. D., "Efficiency Analysis of a Hall Thruster Operating with Krypton and Xenon," AIAA Paper 2005-3638, 2005.

[69]Patel, P., Scheeres, D., Gallimore, A., and Zurbuchen, T., "Automating Trade Studies for Optimal Interplanetary Electric Propulsion Missions," AAS Paper 06-152, 2006.

[70]National Research Council of the National Academies, "Priorities in Space Science Enabled by Nuclear Power and Propulsion," National Academies Press, Washington, DC, 2006, pp. 5–7, 26–29.